Interhemispheric Transport from the Northern Hemisphere Midlatitude Surface

Clara Orbe, Darryn W. Waugh,
Xiaokang Wu, Huang Yang

JOHNS HOPKINS UNIVERSITY

NCAR Asian Monsoon Workshop 03/09/16

What are the transport pathways and timescales that connect the Northern Hemisphere (NH) midlatitude surface (i.e. emissions region for various greenhouse gases (GHGs) and ozone-depleting subtances (ODSs)) to the Southern Hemisphere?

With the exception of a few transport studies (e.g. *Bowman and Erukhimova (2004), Holzer et al. (2009 a,b))*, there is a poor current understanding of the tropospheric transport pathways between the hemispheres and their relationship to large-scale atmospheric dynamics.

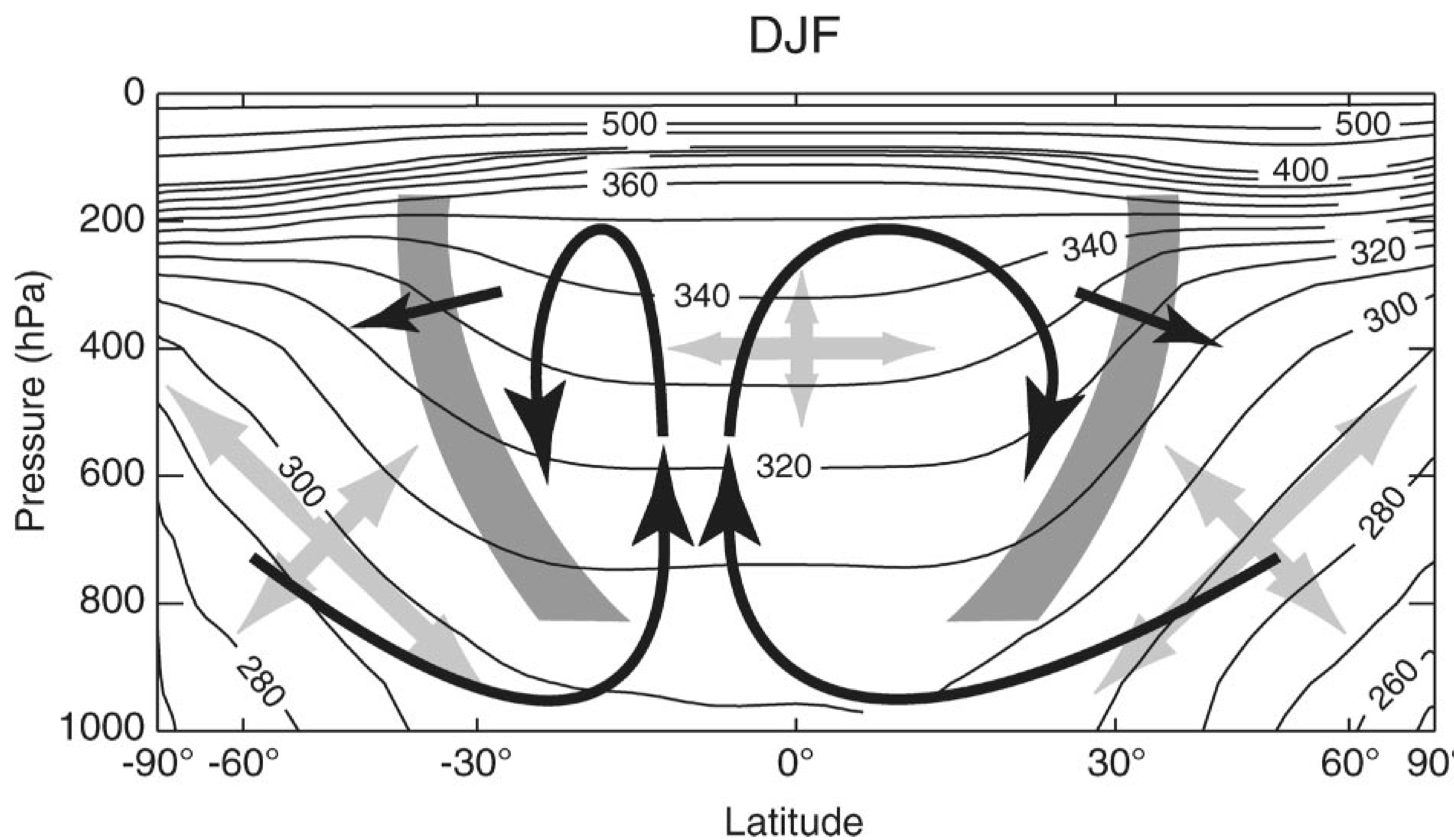

Bowman and Erukhimova (2004)

Most of what we do know quantitatively is limited to gross hemispherically integrated timescales, like the interhemispheric exchange time (τ_{ex}) (e.g., *Geller et al.* (1997), *Gloor et al.* (2007)).

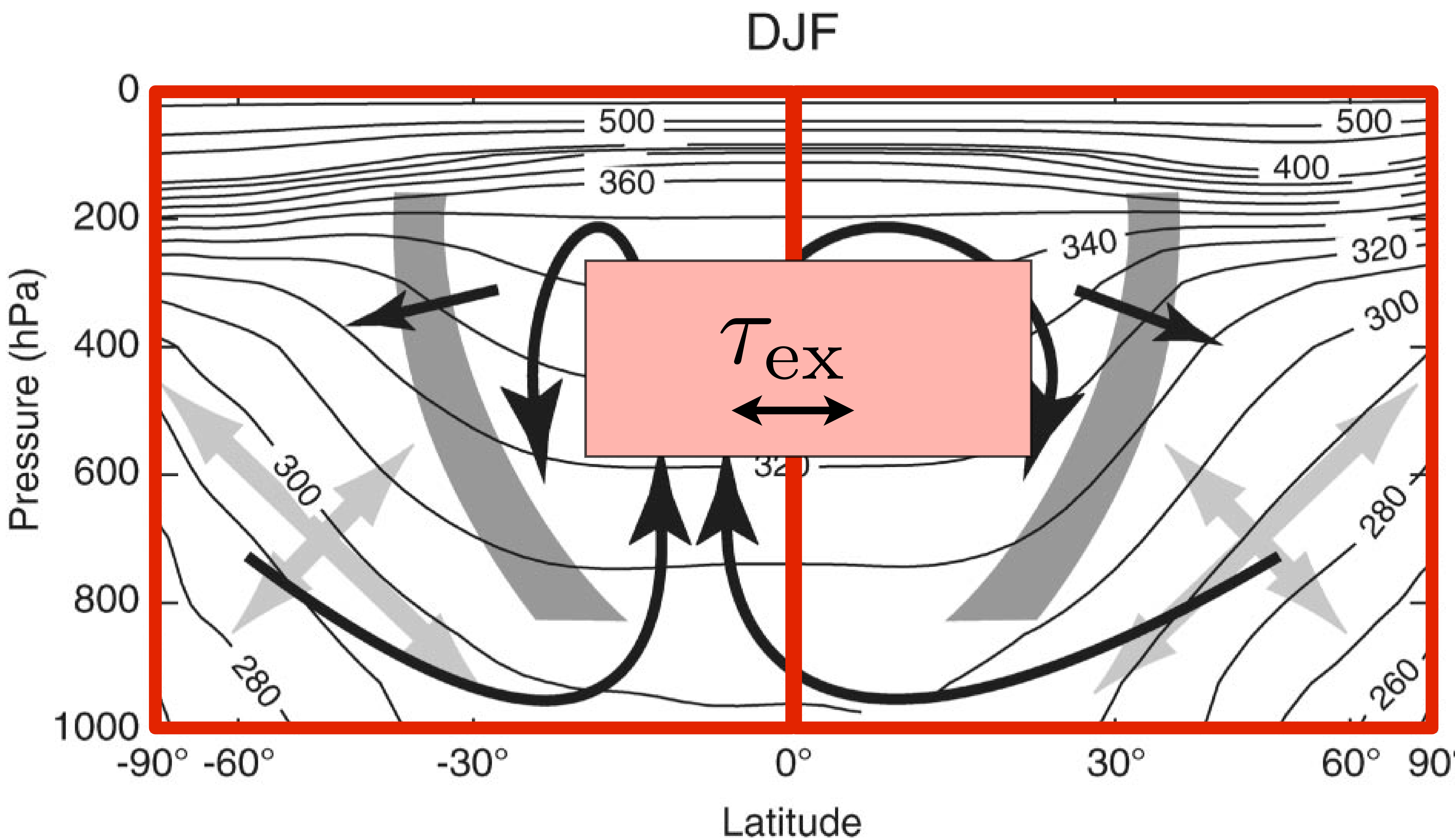

Bowman and Erukhimova (2004)

- However, because of mixing, there is no single timescale that controls transport from a source region (e.g. planetary boundary layer) to the free troposphere, but rather *a distribution of transit times*.
- A natural way to quantify transport for advective-diffusive flows, therefore, is in terms of transit time distributions (TTD).
- TTDs have been used to study ocean surface ventilation [*Wunsch* (2002); *Haine and Hall* (2002)], the oceanic burden of anthropogenic carbon [*Hall et al.* (2004)] and have been used generally as a measure of stratospheric transport [e.g. *Hall and Plumb* (1994)].

More precisely, the TTD is the distribution of transit times ($\tau \equiv t - t'$) since the air at $(\mathbf{r}, t)$ was last at an origin region Ω at time t'.

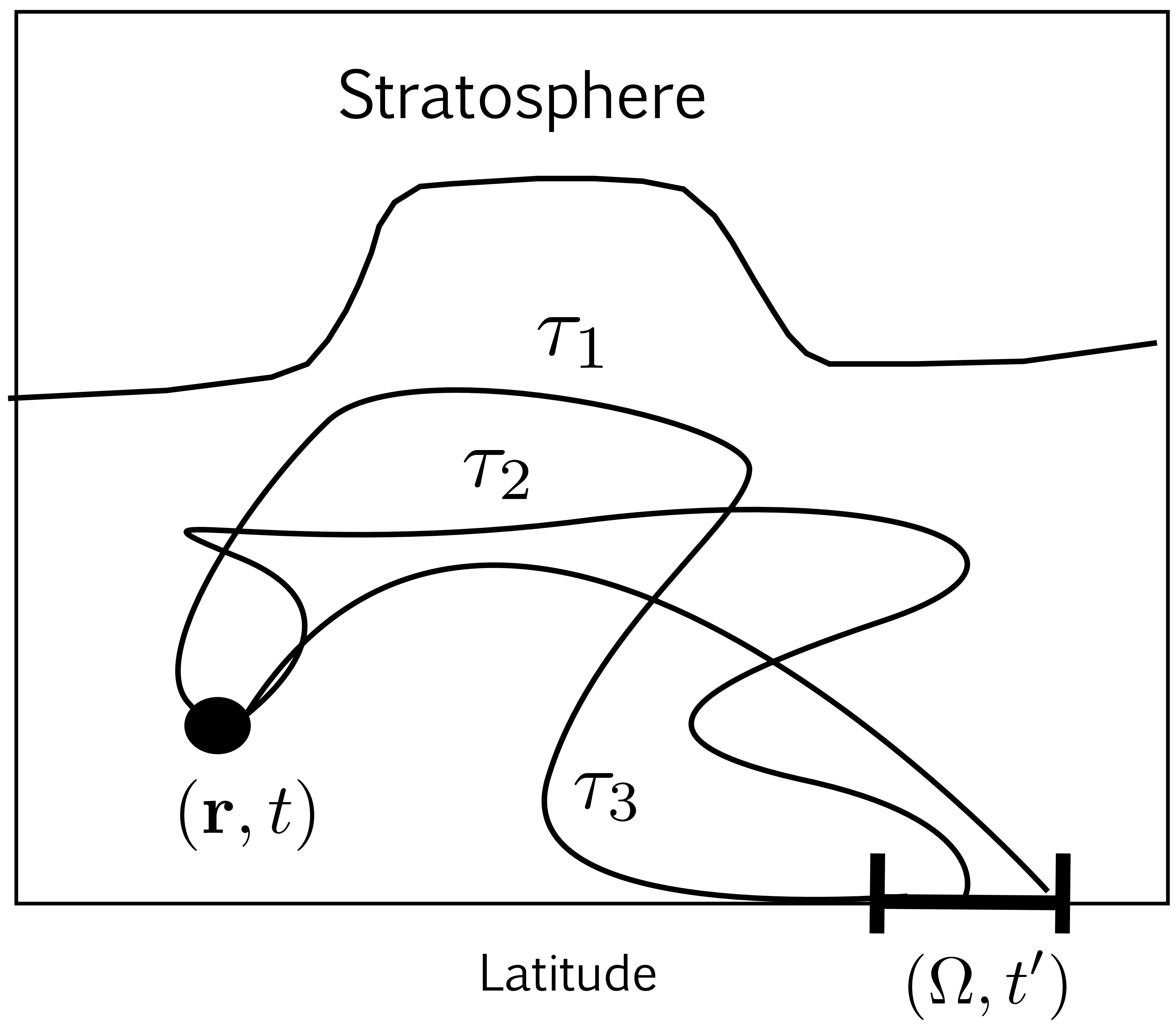

The TTD ($\mathcal{G}(\tau)$) captures the broad range of timescales that connect the origin region Ω (e.g. NH midlatitude surface) to the rest of the atmosphere.

The Transit-Time Distribution (TTD) $\mathcal{G}(\tau)$

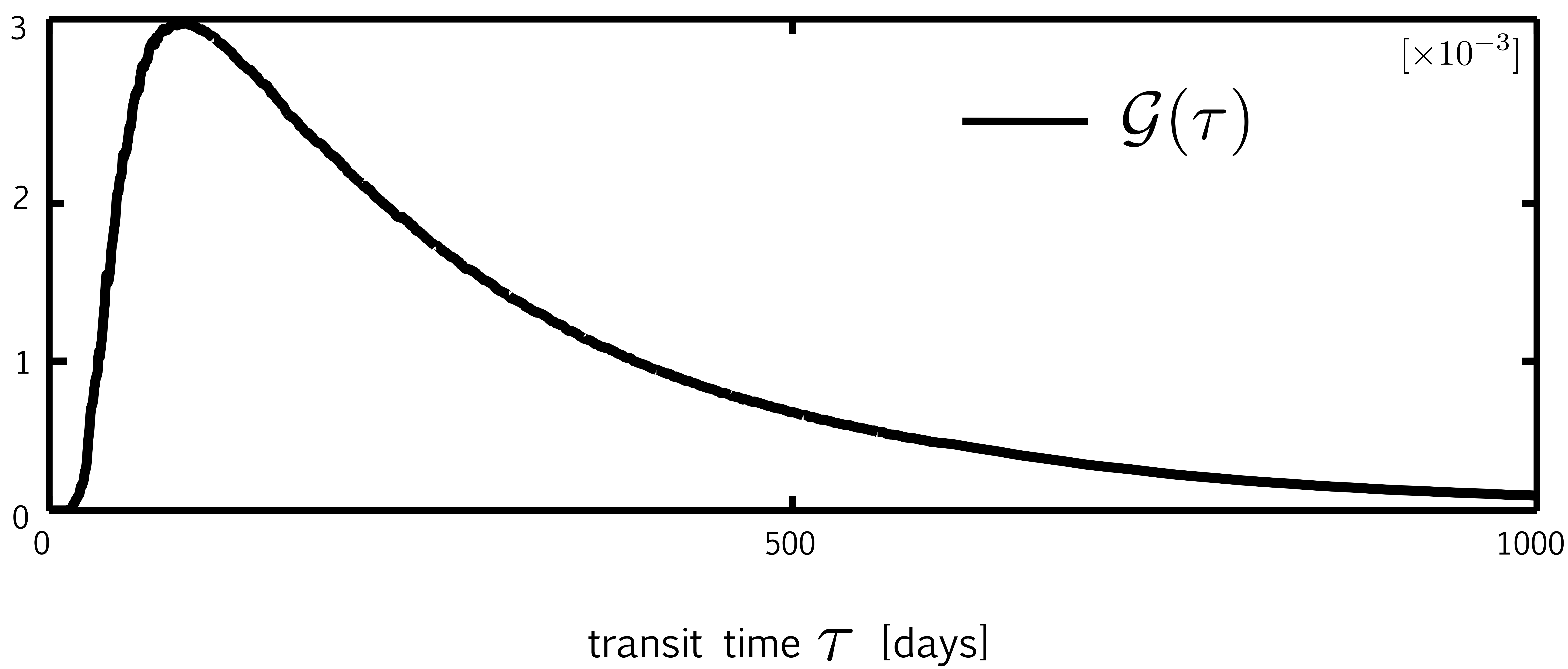

In practice the TTD corresponds to a slice at fixed time t of the Green's function boundary propagator, which can be calculated in models as the solution to:

$$\left(\frac{\partial}{\partial t} + \mathcal{T}\right)\mathcal{G} = 0$$

IC: $\mathcal{G}(\Omega, t, t') = \delta(t - t')$

Zero flux BC conditions elsewhere. The transport operator, $\mathcal{T}$, is defined as:

$$\mathcal{T} = \mathbf{v} \cdot \nabla\chi - \rho^{-1}\nabla \cdot (\rho\kappa\nabla\chi)$$

All of the air at $(\mathbf{r}, t)$ had to have last contacted Ω sometime in its history:

$$\int_0^\infty d\tau \mathcal{G}(\mathbf{r}, t, \tau | \Omega) = 1$$

[*Holzer and Hall* (2000)]

In practice the TTD corresponds to a slice at fixed time t of the Green's function boundary propagator, which can be calculated in models as the solution to:

$$(\frac{\partial}{\partial t} + \mathcal{T})\mathcal{G} = 0$$

IC: $\mathcal{G}(\Omega, t, t') = \delta(t - t')$

Zero flux BC conditions elsewhere. The transport operator, $\mathcal{T}$, is defined as:

$$\mathcal{T} = \mathbf{v} \cdot \nabla\chi - \rho^{-1}\nabla \cdot (\rho\kappa\nabla\chi)$$

Eulerian Approach:

Model: NASA GMI-CTM (*Strahan et al. (2007)*) driven with MERRA reanalysis fields (2000-2010).

TTD: Approximate the TTD ($\mathcal{G}$) as the average of an ensemble of four Boundary Impulse Response (i.e. "pulse") passive tracers (e.g. *Haine et al. (2008), Li et al. (2012)*) that are released at the NH midlatitude surface at times t' = January 1, April 1, July 1 and October 1 in year 2000.

Quick Note on BIR-based Approximation of the TTD

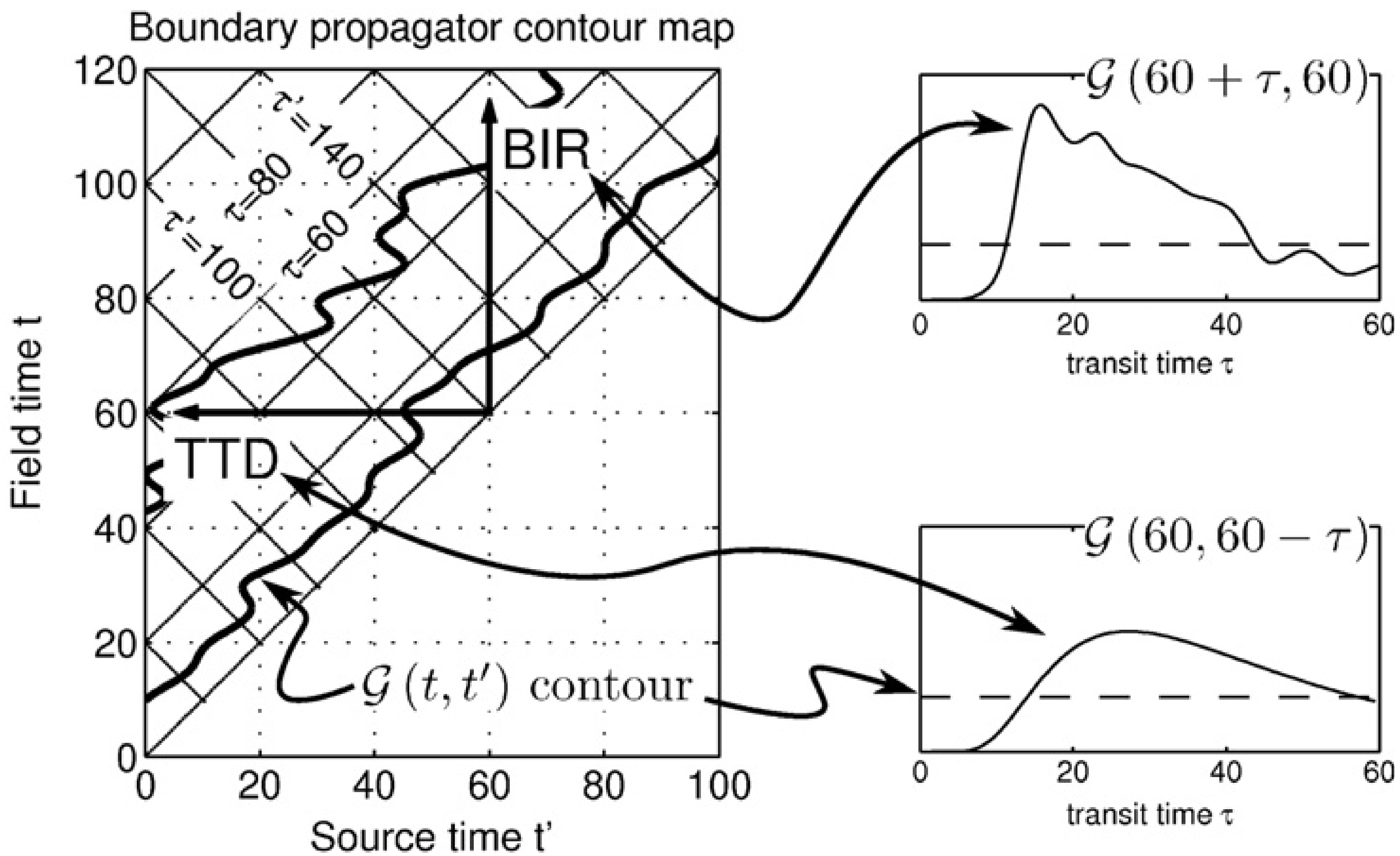

From *Haine et al. (2008)*

- For non-stationary flow the BIR (boundary impulse response) *does not* equal the TTD
- However, the statistics of the BIR and the TTD (i.e. temporal moments) are the same (*Haine et al. (2008)*).
- The fidelity of other properties of the TTD (i.e. modal transit times) are assessed used idealized loss tracers.

Model calculations and observational inferences of the TTD in the stratosphere have shown that the TTD, $\mathcal{G}(\tau)$, is very broad [*Hall and Plumb (1994), Waugh and Hall (2002)]*.

The Transit-Time Distribution (TTD) $\mathcal{G}(\tau)$

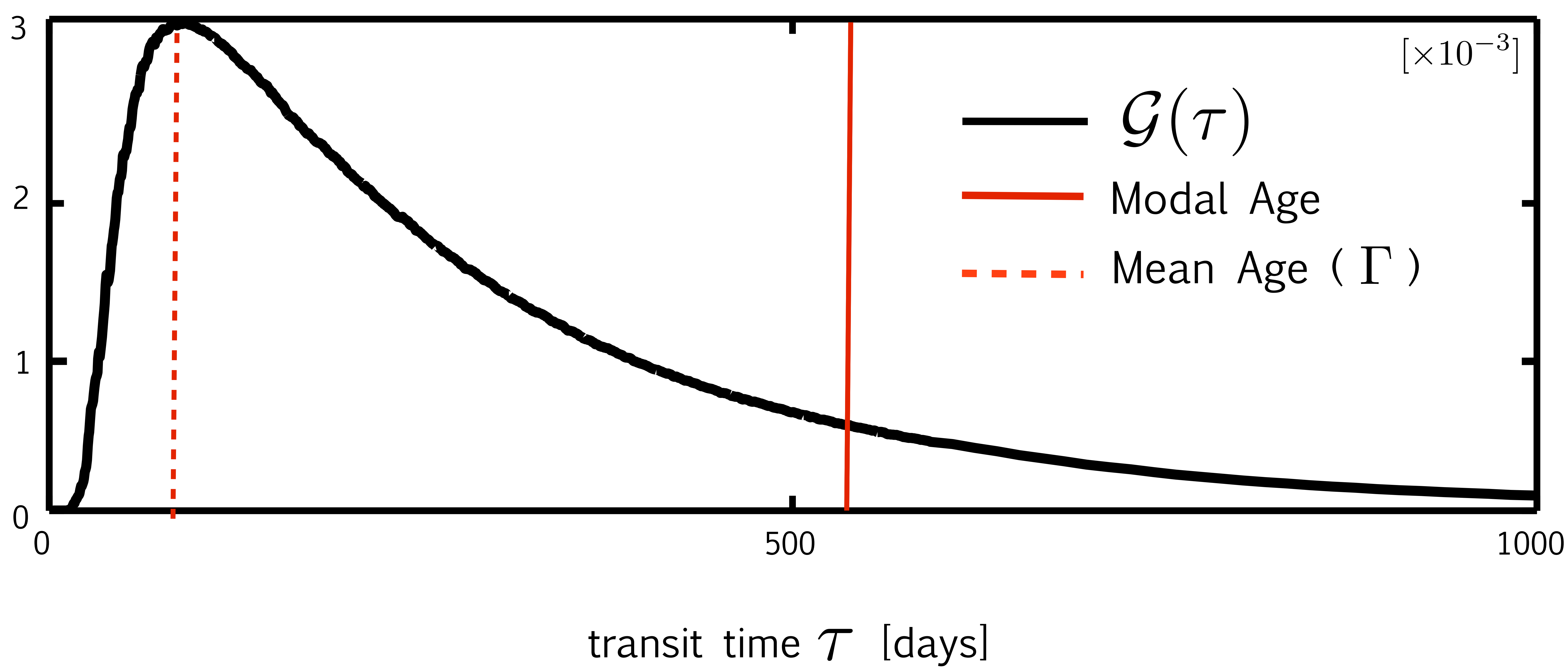

TTD in GMI-MERRA Simulation

Transit-Time Distribution $\mathcal{G}(\mathbf{r}, \tau | \Omega_{\mathrm{MID}})$
at 312 hPa (top) and 873 hPa (bottom)

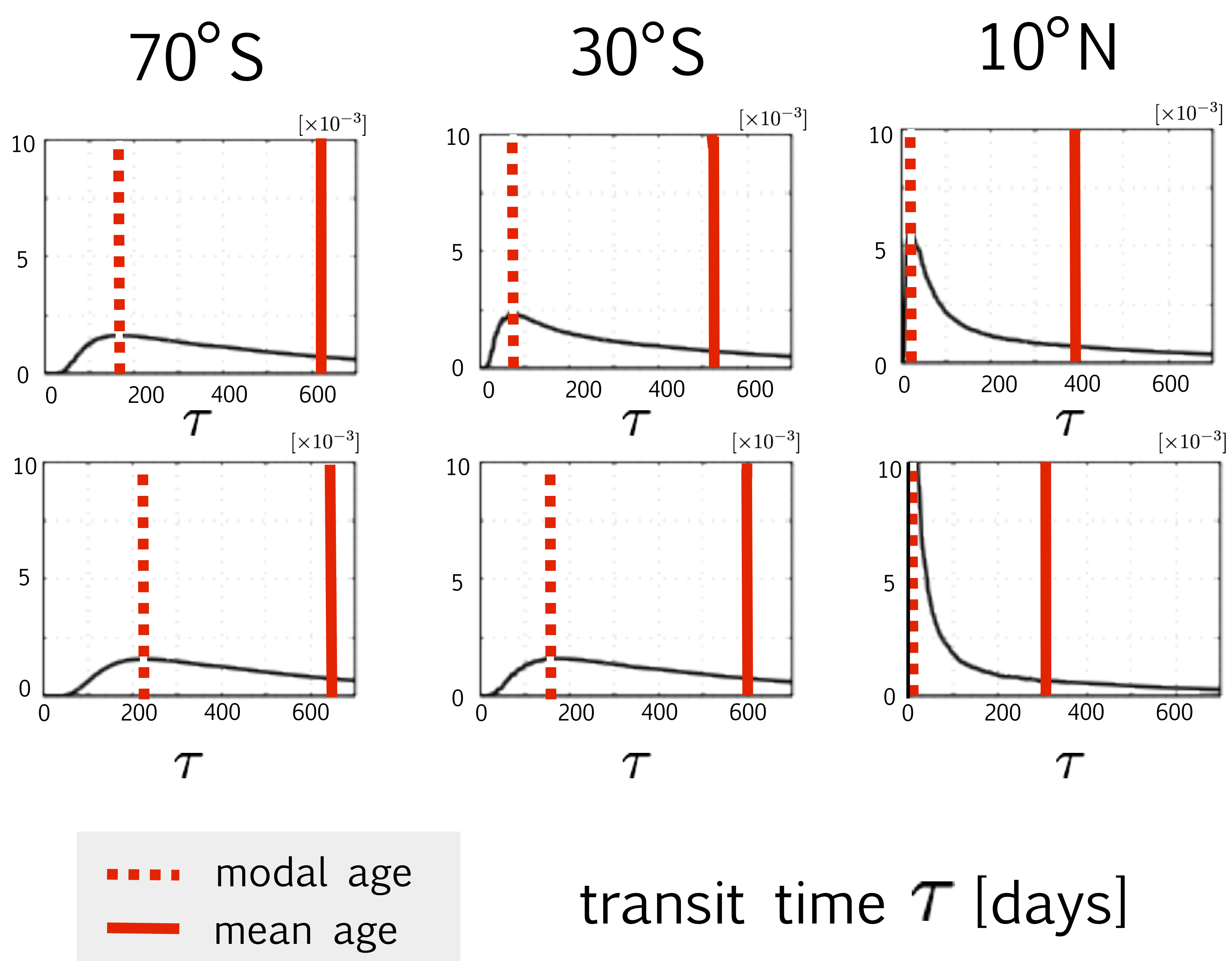

The GMI-MERRA TTD approximation shows that there is also a broad range of transport timescales throughout the troposphere.

Here, the source region $\Omega_{\mathrm{MID}} \equiv$ Northern Hemisphere midlatitude surface (i.e. first model level between 30°N-50°N)

[Orbe et al. (2015), Submitted]

TTD in GMI-MERRA Simulation

Transit-Time Distribution $\mathcal{G}(\mathbf{r}, \tau | \Omega_{\mathrm{MID}})$

at 312 hPa (top) and 873 hPa (bottom)

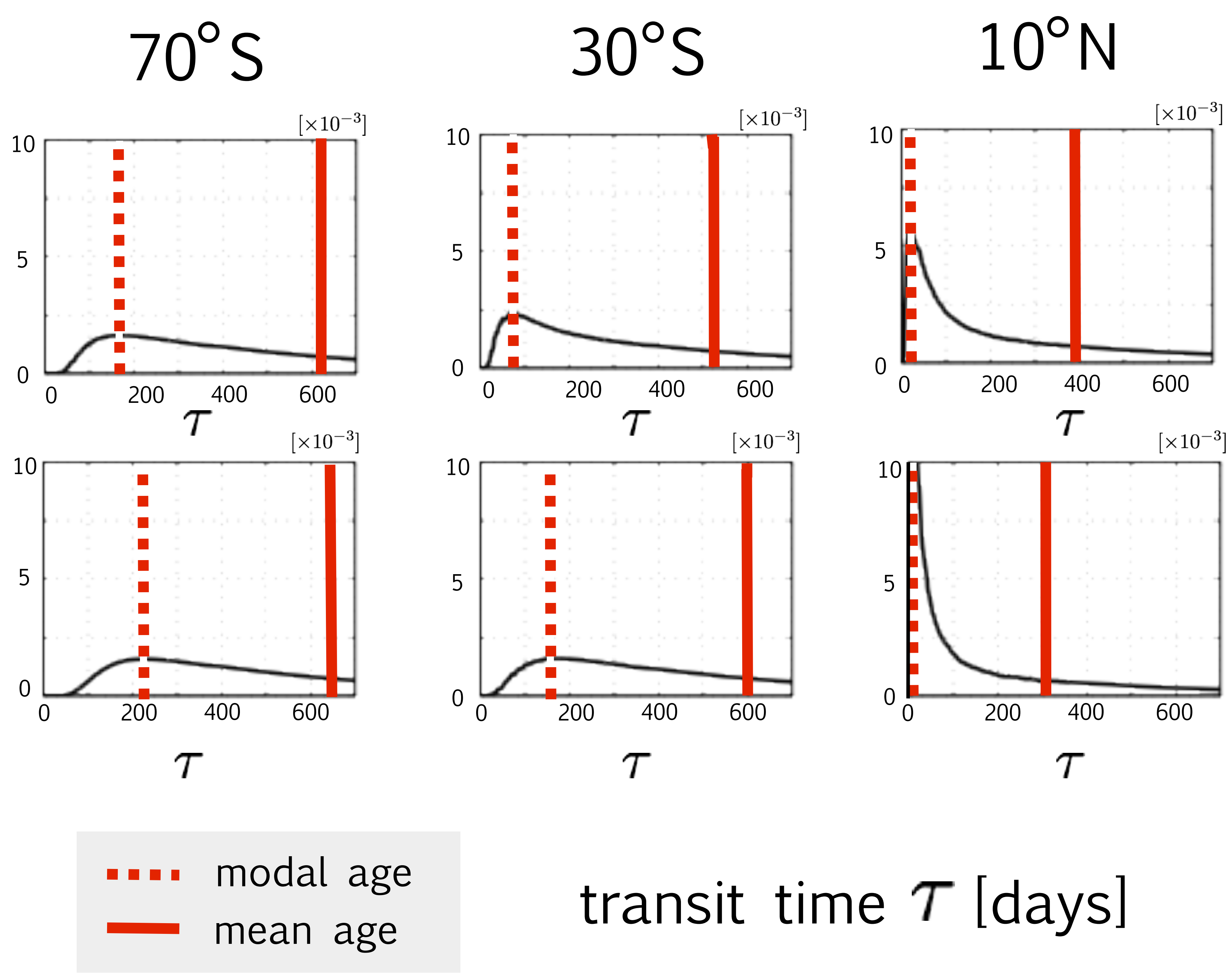

transit time τ [days]

These results strongly indicate that a single interhemispheric exchange time (τ_{ex}) does not capture the broad range of transport paths and timescales that determine the distributions of greenhouse gases and ozone-depleting substances.

[Orbe et al. (2015), Submitted]

Mean Age: Model vs. Observations

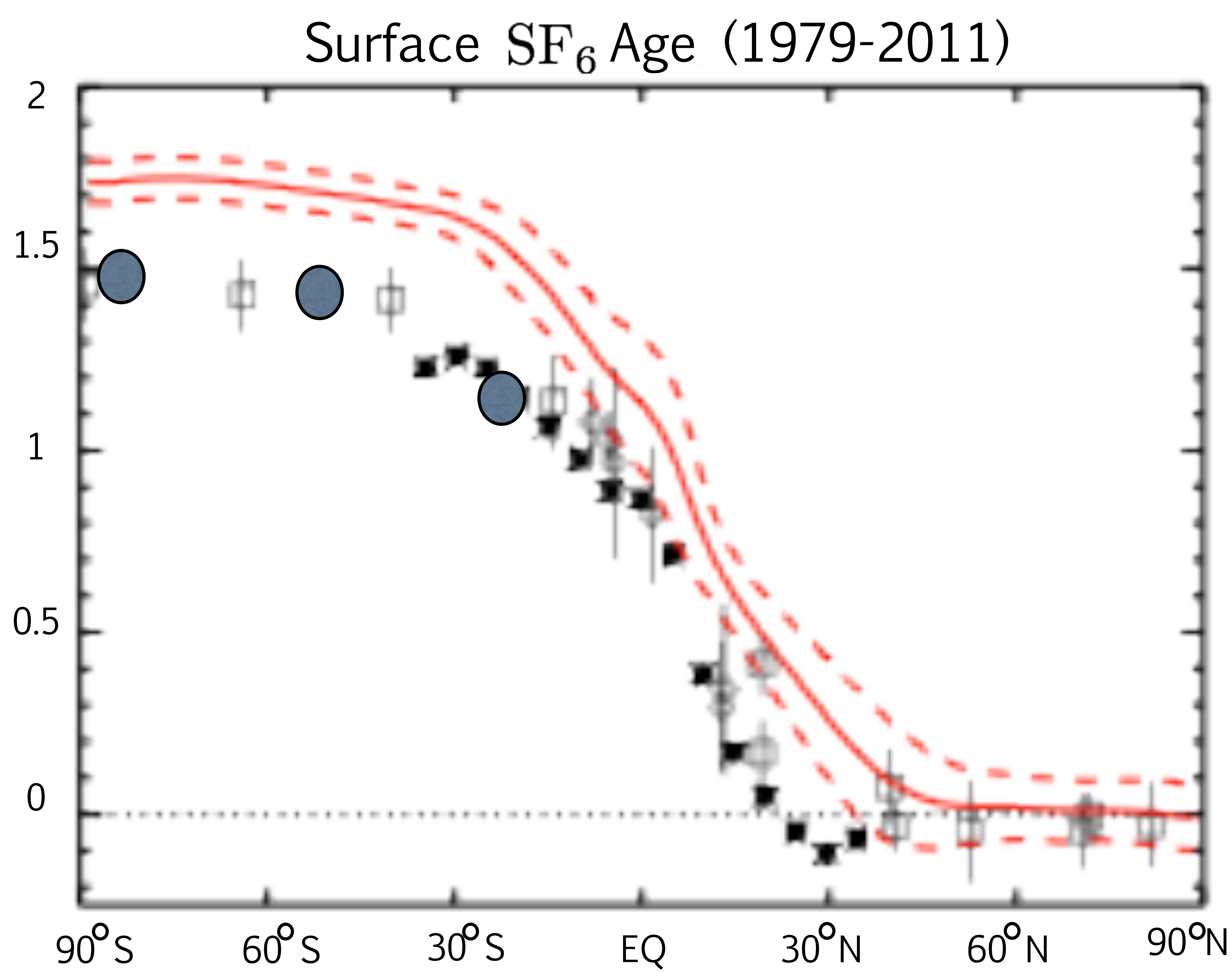

From *Waugh et al. (2013)*

Modeled interhemispheric transport is slightly slow, compared to observations, where SF_6 age (Γ_{SF6}) is equal to the mean age and is defined as:

$$\chi_{SF6}(\mathbf{r}, t) = \chi_0(t - \Gamma_{SF6})$$

□ ◇ ✱ (HATS, CCGG, ship cruise SF_6)

● (HATS SF_6, CFCs, HCFCs) from *Holzer and Waugh (2015)*

— surface SF_6 age at 180°W from GMI-MERRA model (± 1 standard deviation)

Main Properties of the TTD

#1 Mean transit times (i.e. mean ages) are much larger than their corresponding modal transit times (i.e. modal ages).

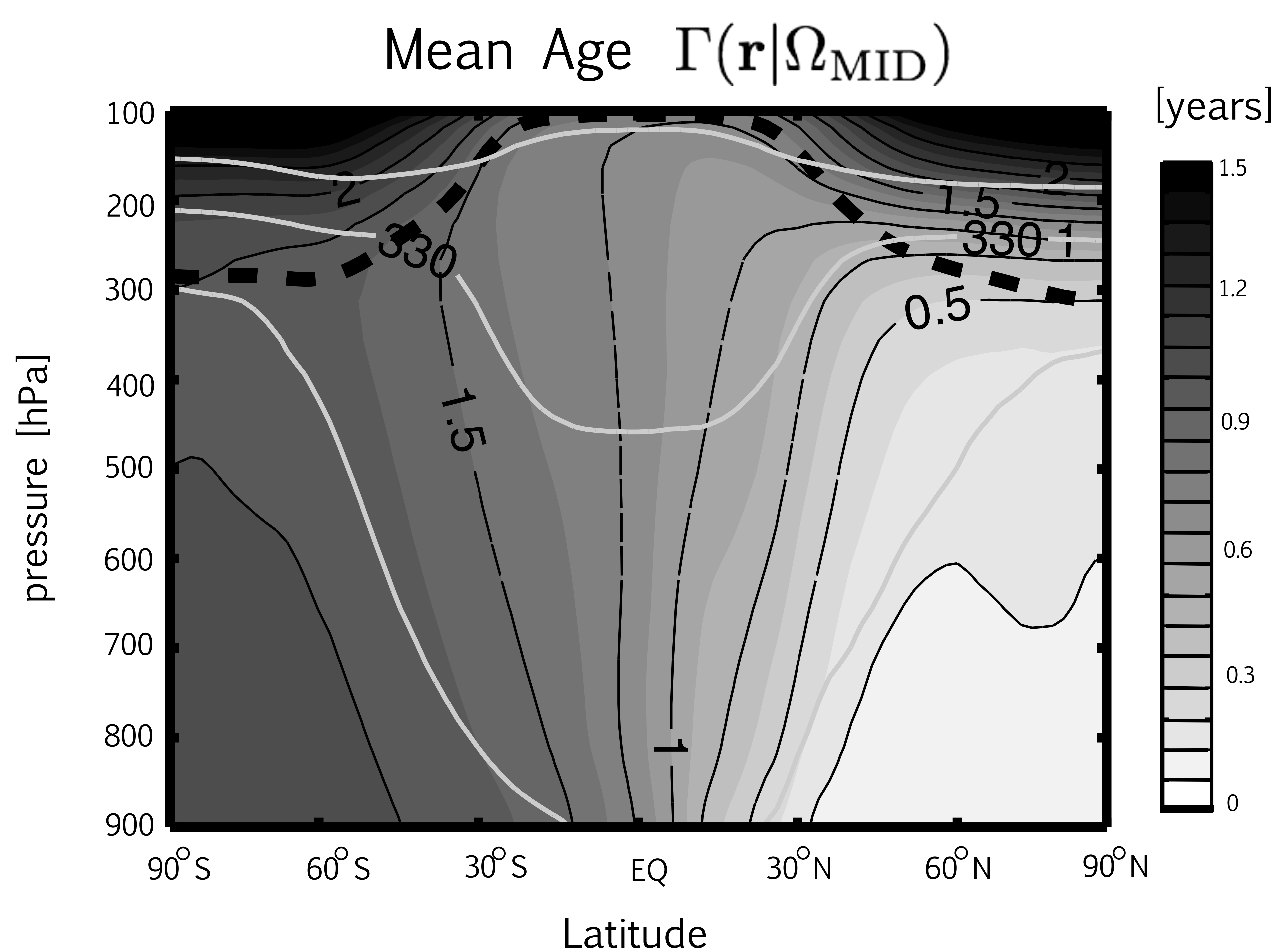

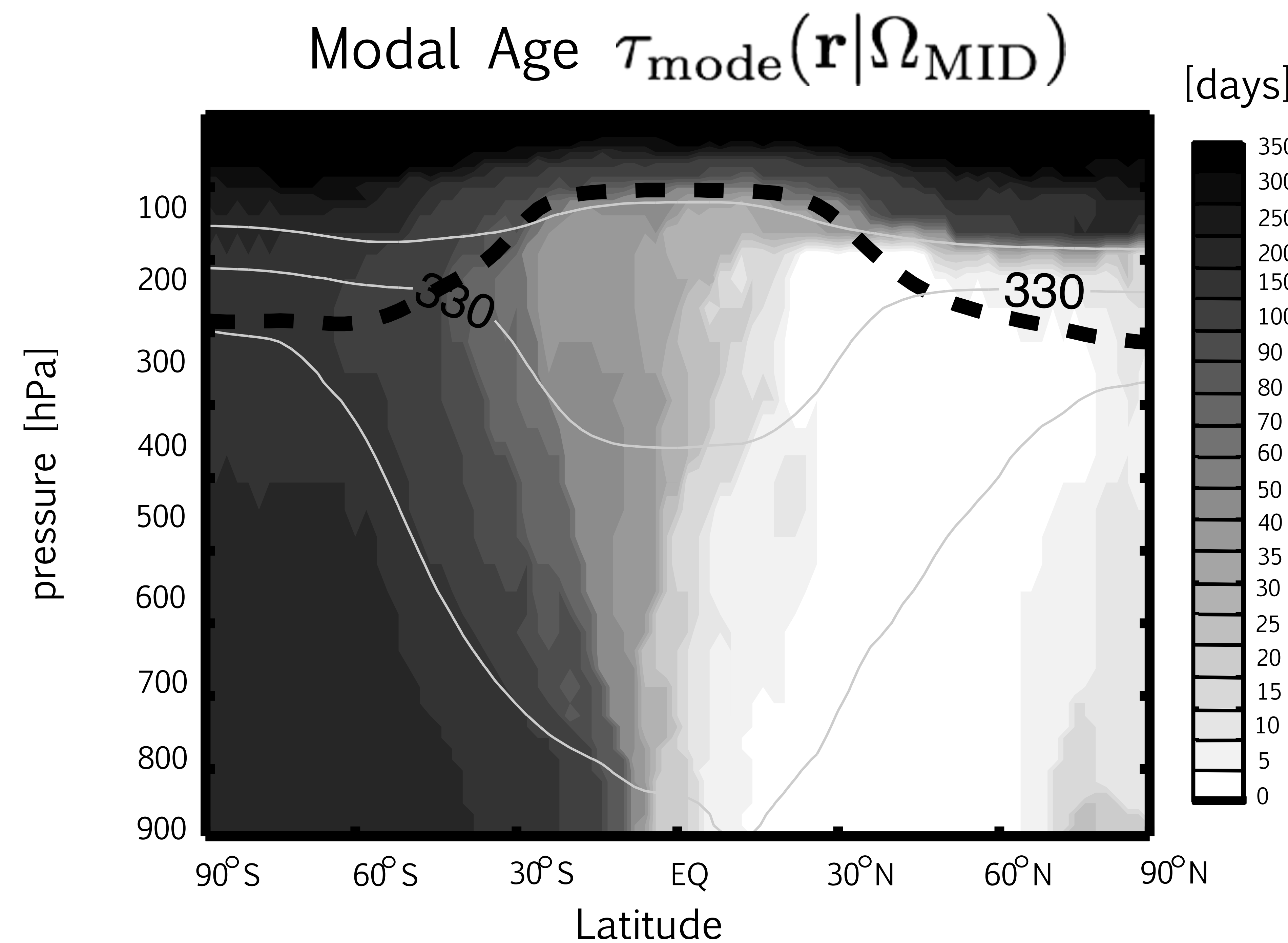

Main Properties of the TTD

#2 The shape of the TTD changes throughout the troposphere. The TTD is broader relative to its mean in the tropical upper troposphere (i.e. more skewed/asymmetric).

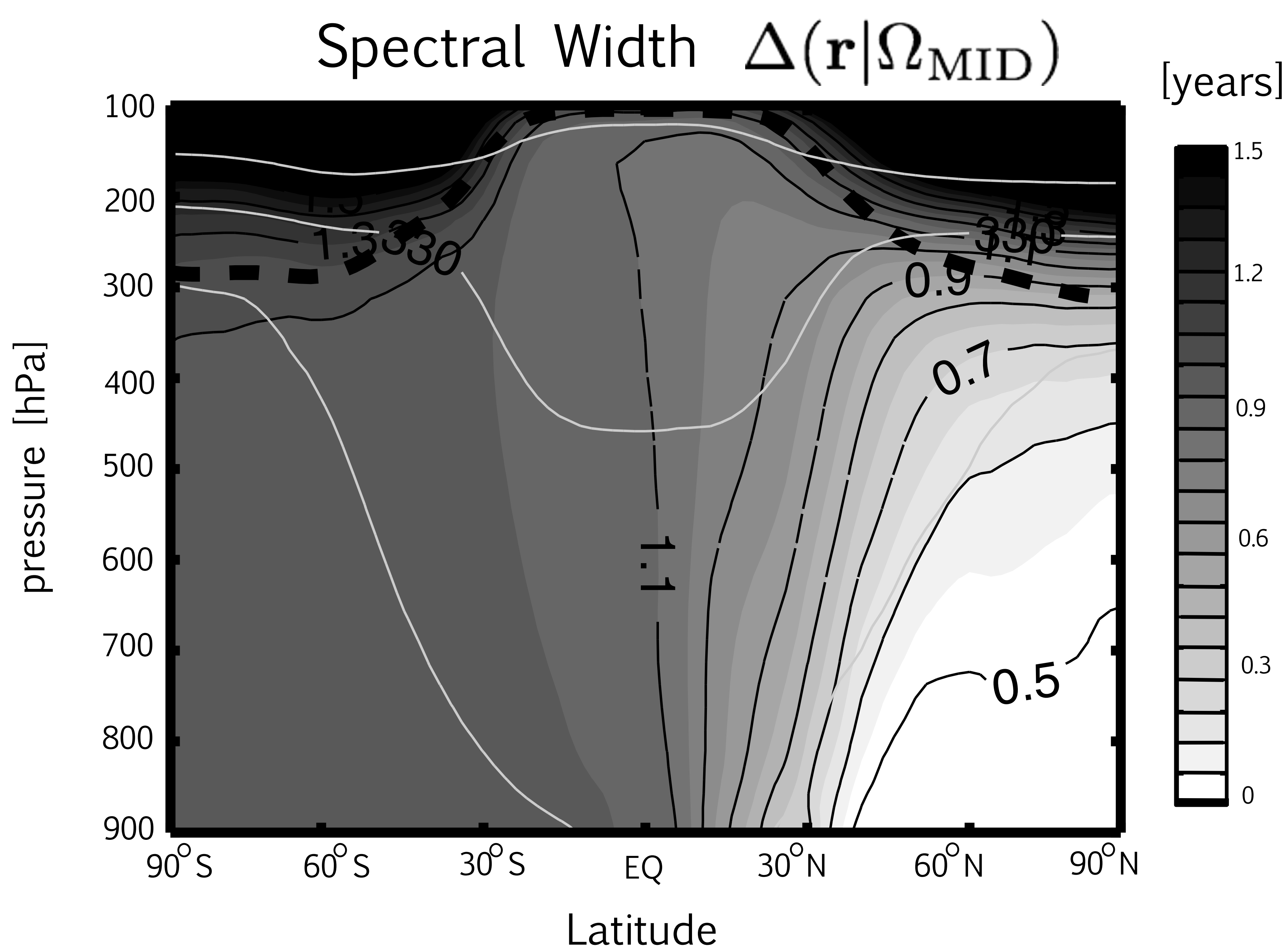

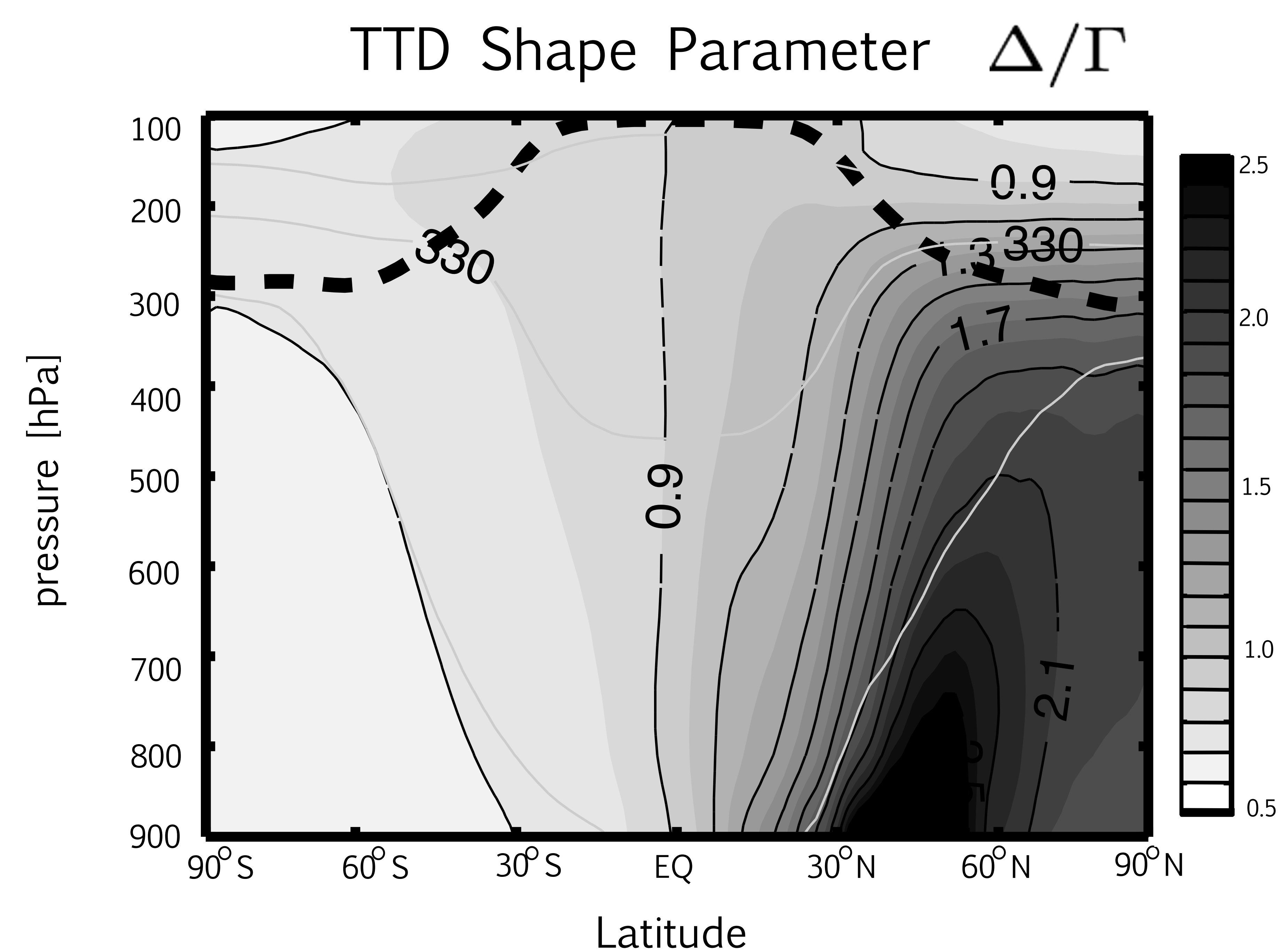

Main Properties of the TTD

#2 The shape of the TTD changes throughout the troposphere. The TTD is broader relative to its mean in the tropical upper troposphere (i.e. more skewed/asymmetric).

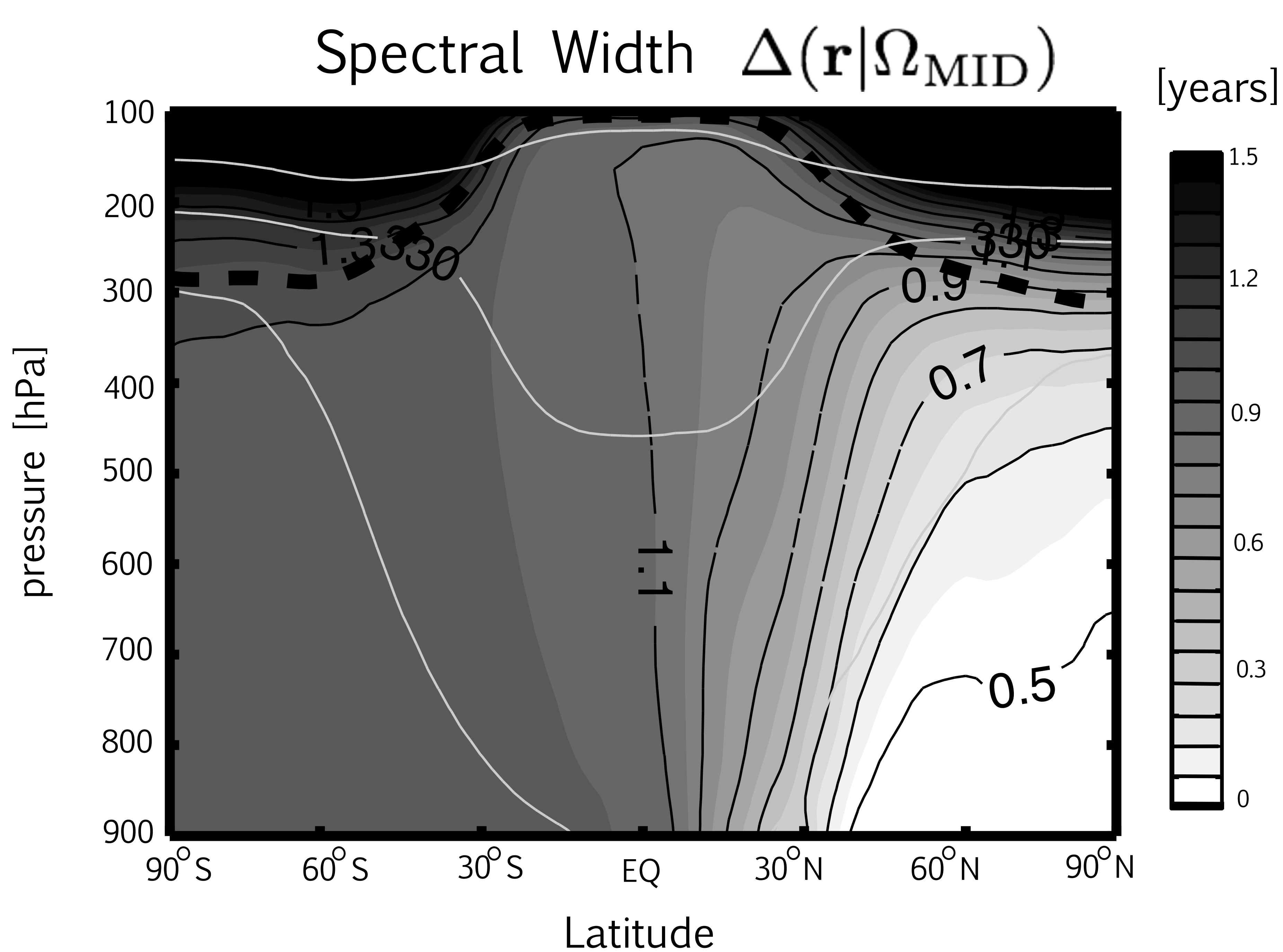

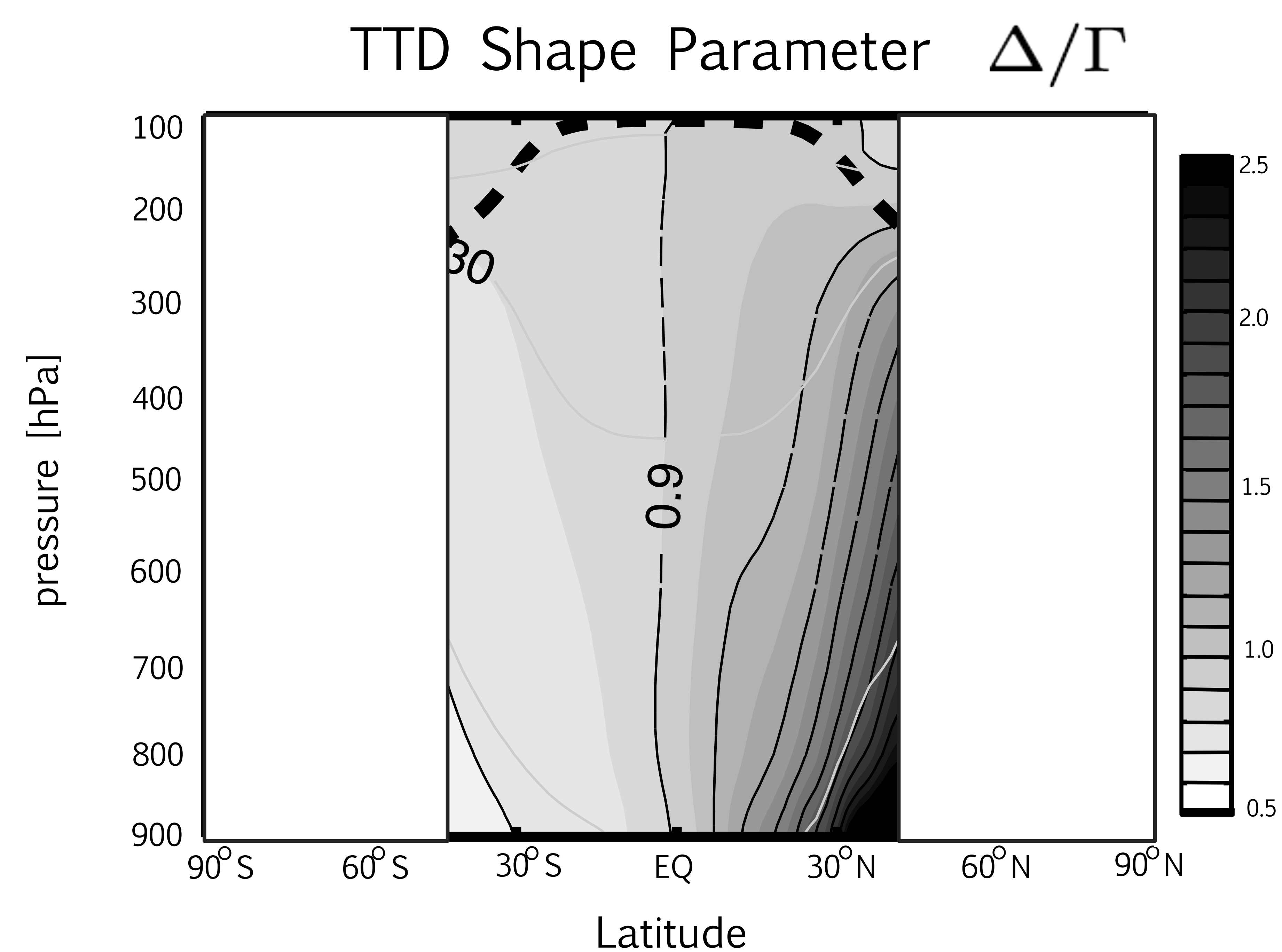

Main Properties of the TTD

#2 The shape of the TTD changes throughout the troposphere. The TTD is broader relative to its mean in the tropical upper troposphere (i.e. more skewed/asymmetric).

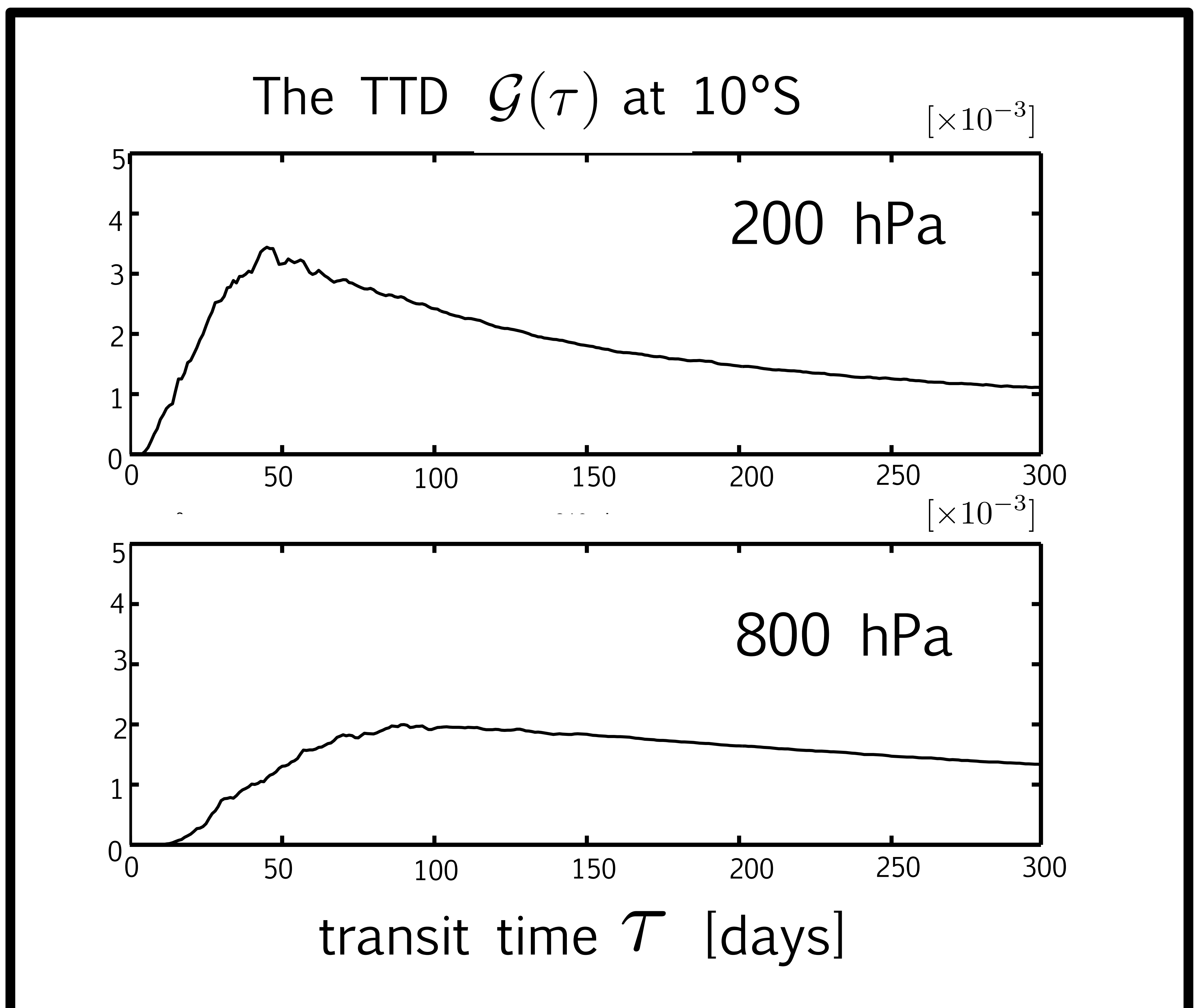

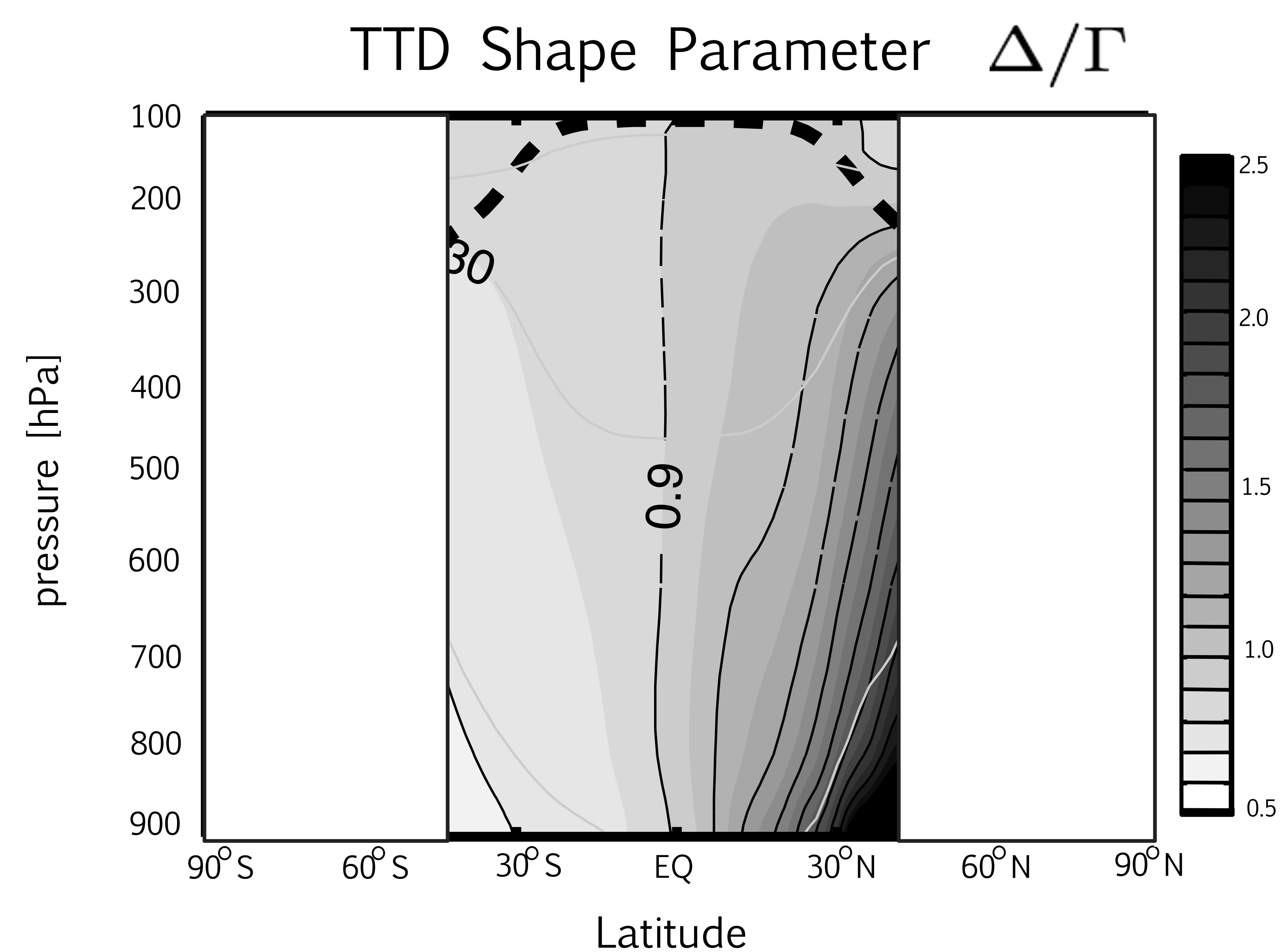

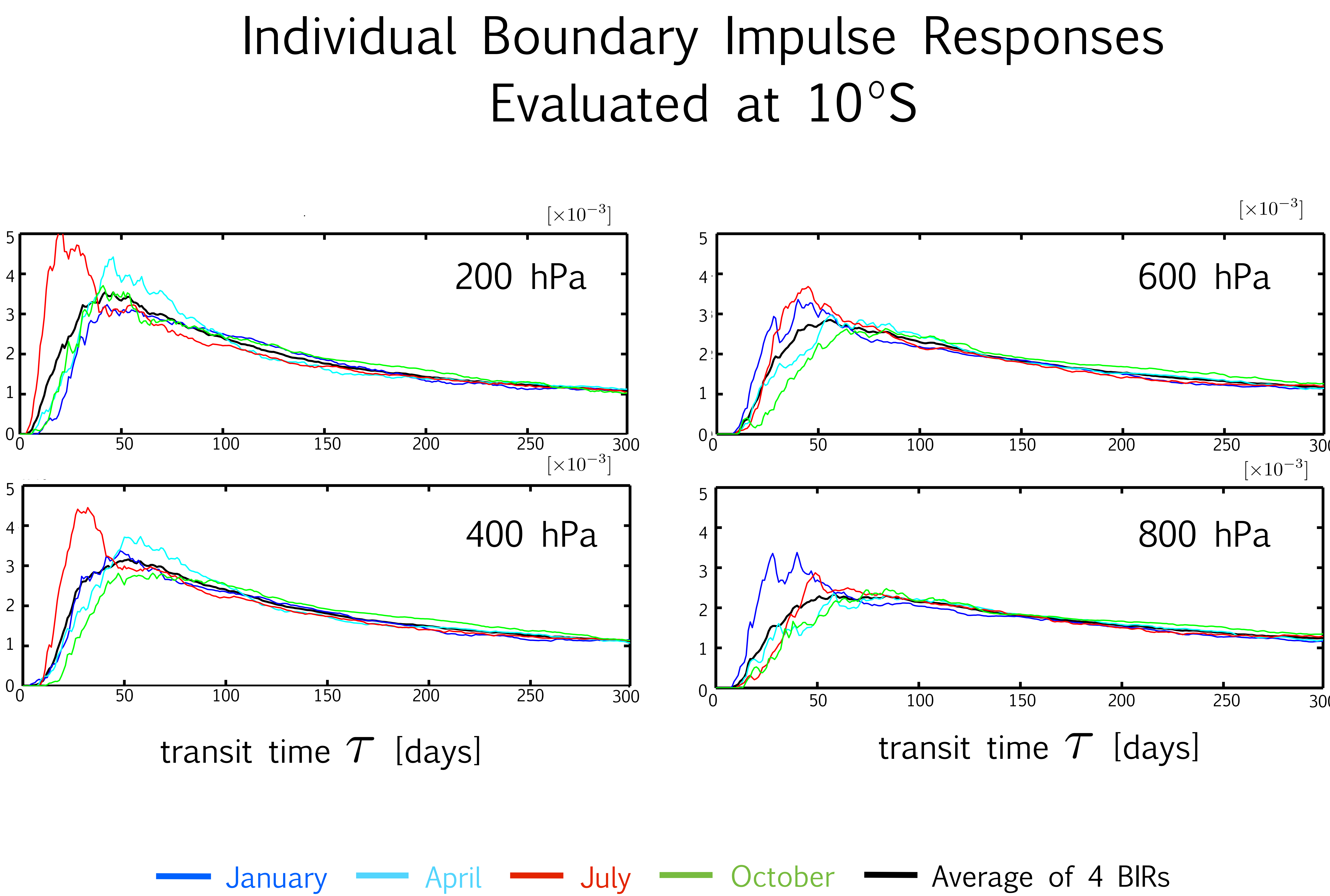
Individual Boundary Impulse Responses
Evaluated at 10°S
200 hPa
400 hPa
600 hPa
800 hPa
[×10⁻³]
transit time τ [days]
January
April
July
October
Average of 4 BIRs

Individual Boundary Impulse Responses Evaluated at 10°S

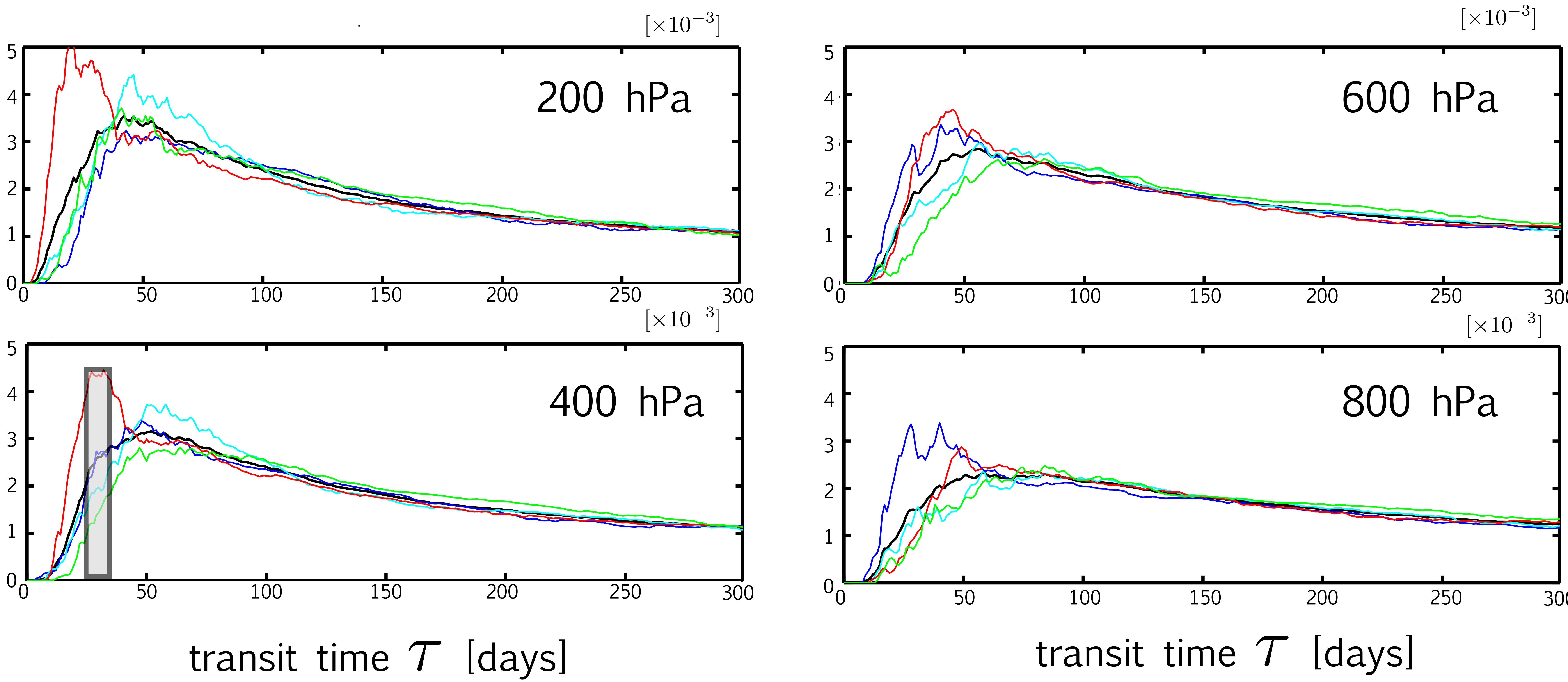

Define a BIR "fraction" $f_{\tau_1}^{\tau_2}(\mathbf{r}|\Omega_{\mathrm{MID}}, t') \equiv \int_{\tau_1}^{\tau_2} \mathcal{G}(\mathbf{r}, t|\Omega_{\mathrm{MID}}, t')$

Percentage of Air that was Last at Ω_{MID} 1-10 Days Ago

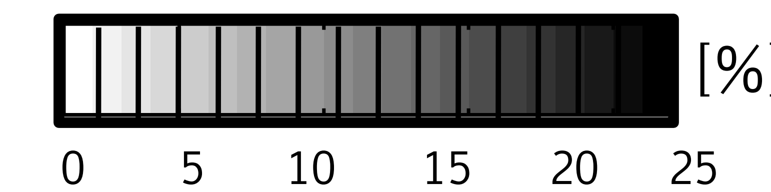

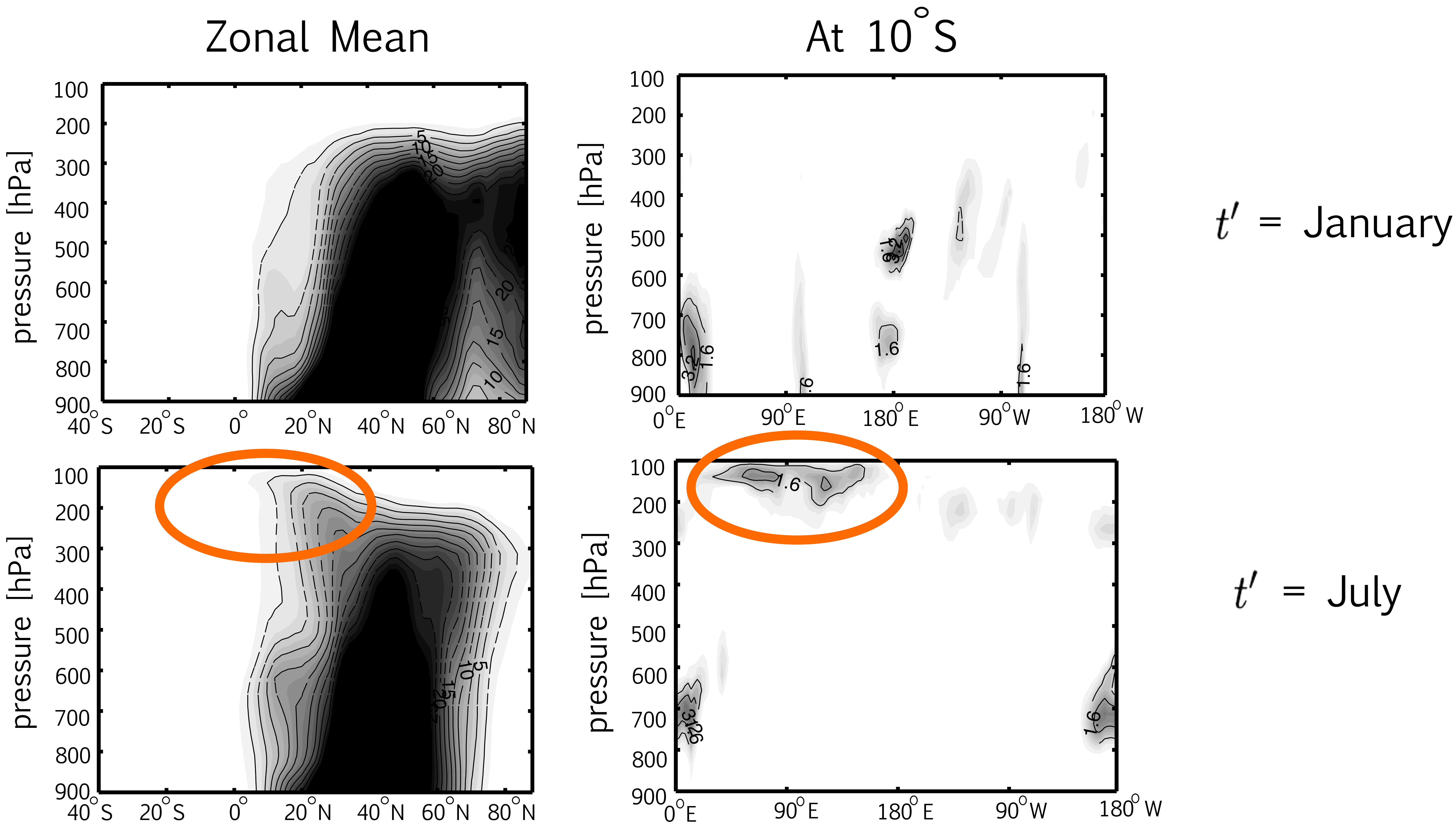

Percentage of Air that was Last at Ω_{MID} 11-20 Days Ago

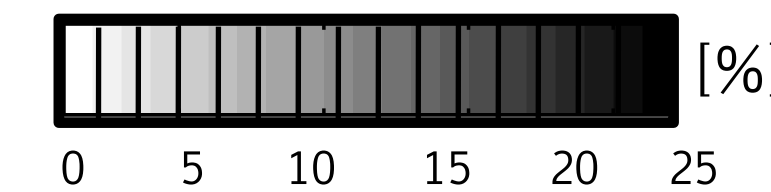

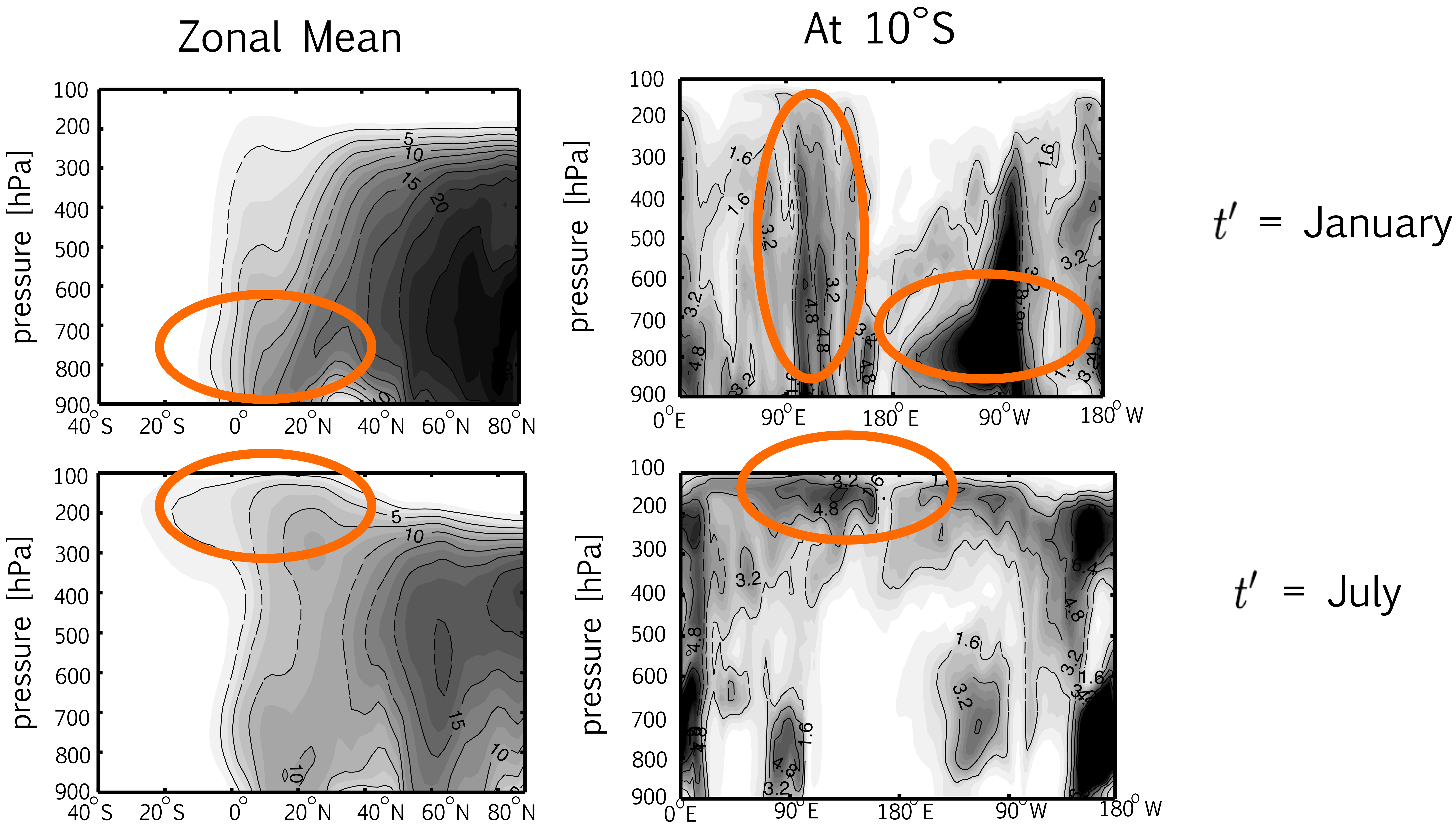

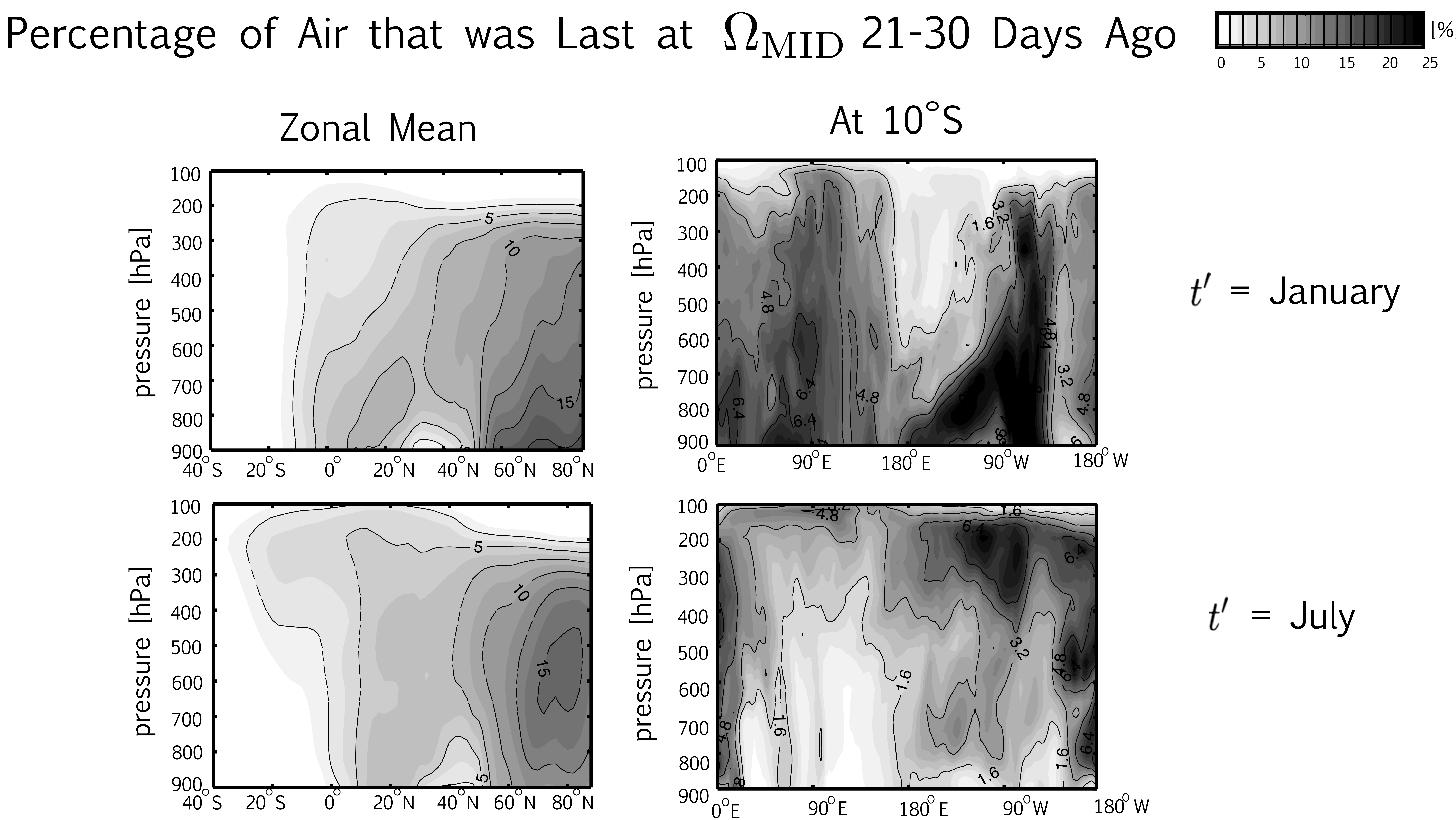
Percentage of Air that was Last at Ω_{MID} 21-30 Days Ago
[%]
0 5 10 15 20 25
Zonal Mean
At 10°S
t' = January
t' = July
pressure [hPa]
100 200 300 400 500 600 700 800 900
40°S 20°S 0° 20°N 40°N 60°N 80°N
0°E 90°E 180°E 90°W 180°W
5
10
15
1.6
3.2
4.8
6.4

Percentage of Air that was Last at Ω_{MID} 31-40 Days Ago

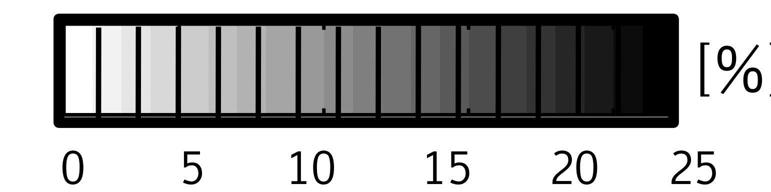

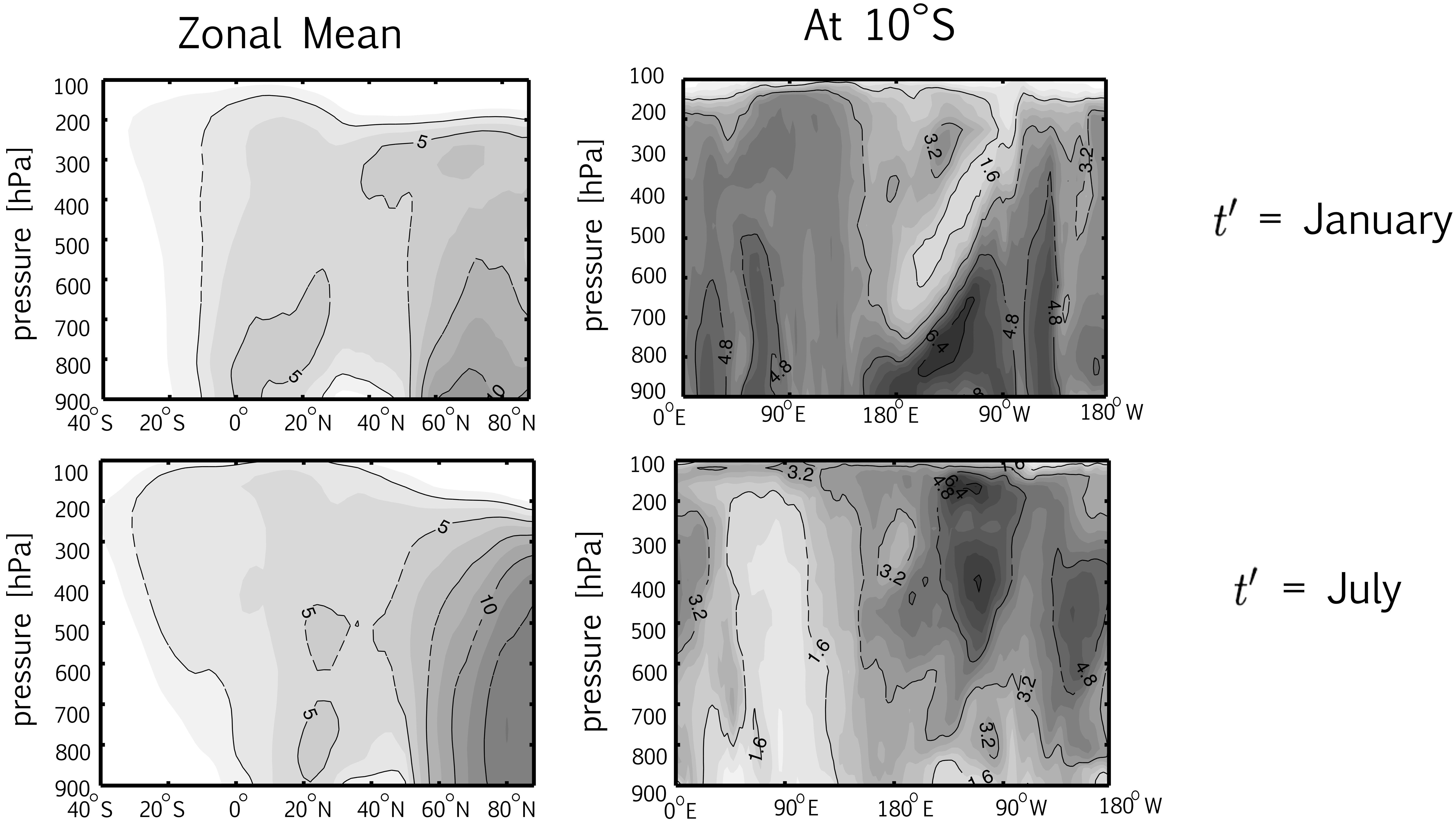

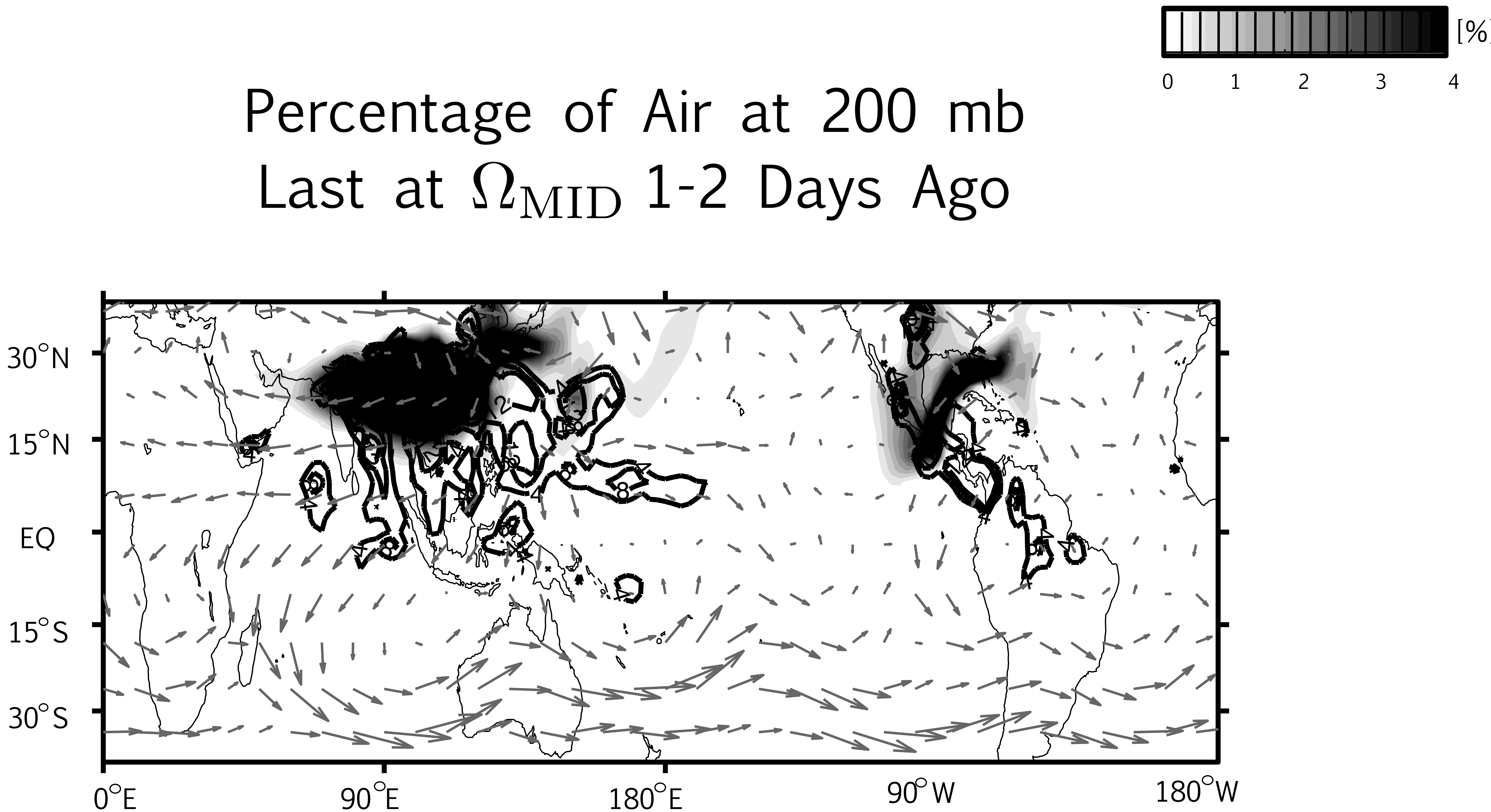

Shading: BIR fraction $f_{\tau_1}^{\tau_2}(\mathbf{r}|\Omega_{\mathrm{MID}}, t')$
Black contours: cumulative mass flux from convection $[\times 10^{-3}\ \mathrm{kg/m^2/s}]$
Winds: MERRA Reanalysis

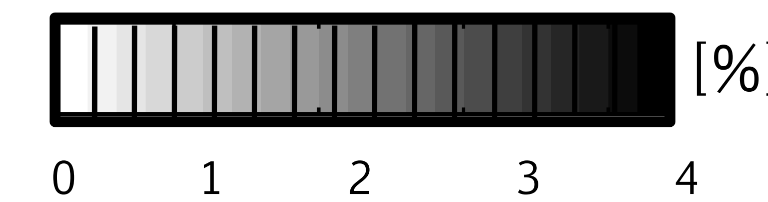

Percentage of Air at 200 mb Last at Ω_{MID} 3-4 Days Ago

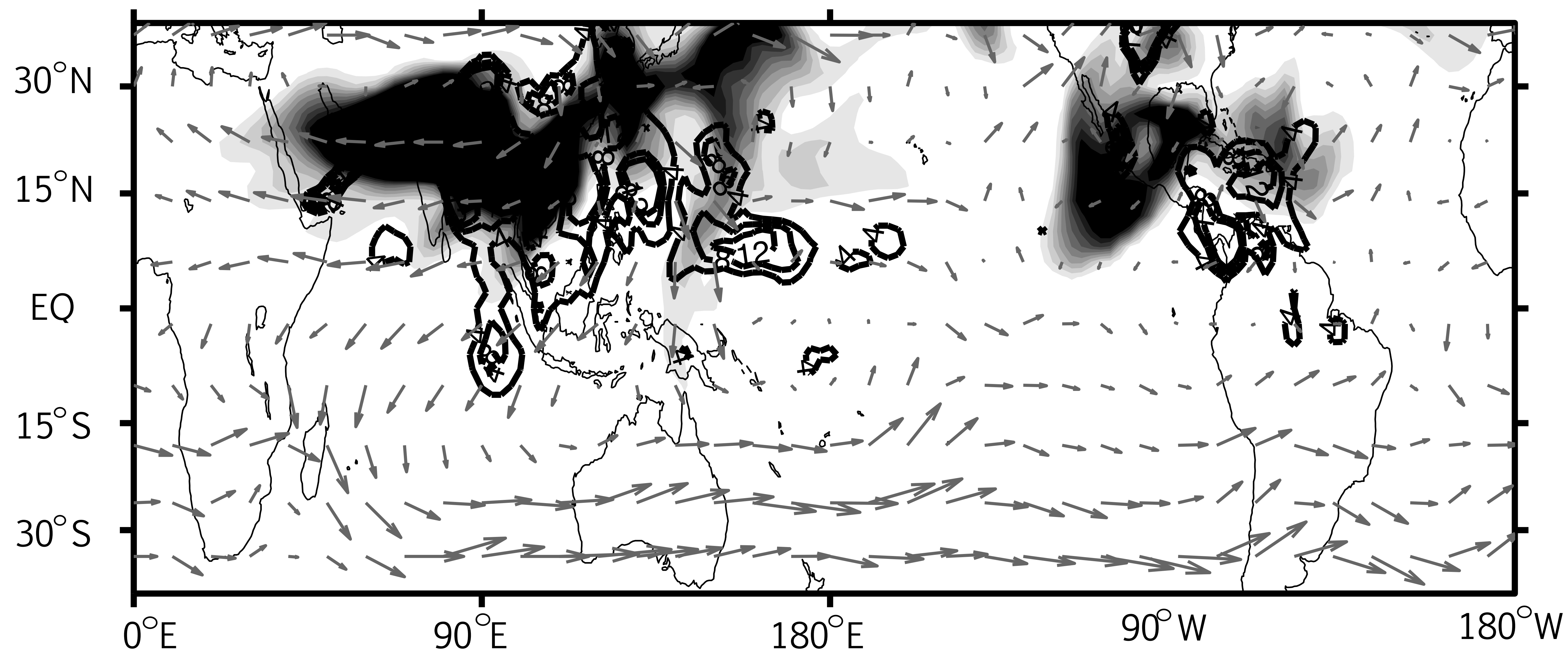

Shading: BIR fraction $f_{\tau_1}^{\tau_2}(\mathbf{r}|\Omega_{\mathrm{MID}}, t')$
Black contours: cumulative mass flux from convection $[\times 10^{-3}\ \mathrm{kg/m^2/s}]$
Winds: MERRA Reanalysis

Percentage of Air at 200 mb Last at Ω_{MID} 5-6 Days Ago

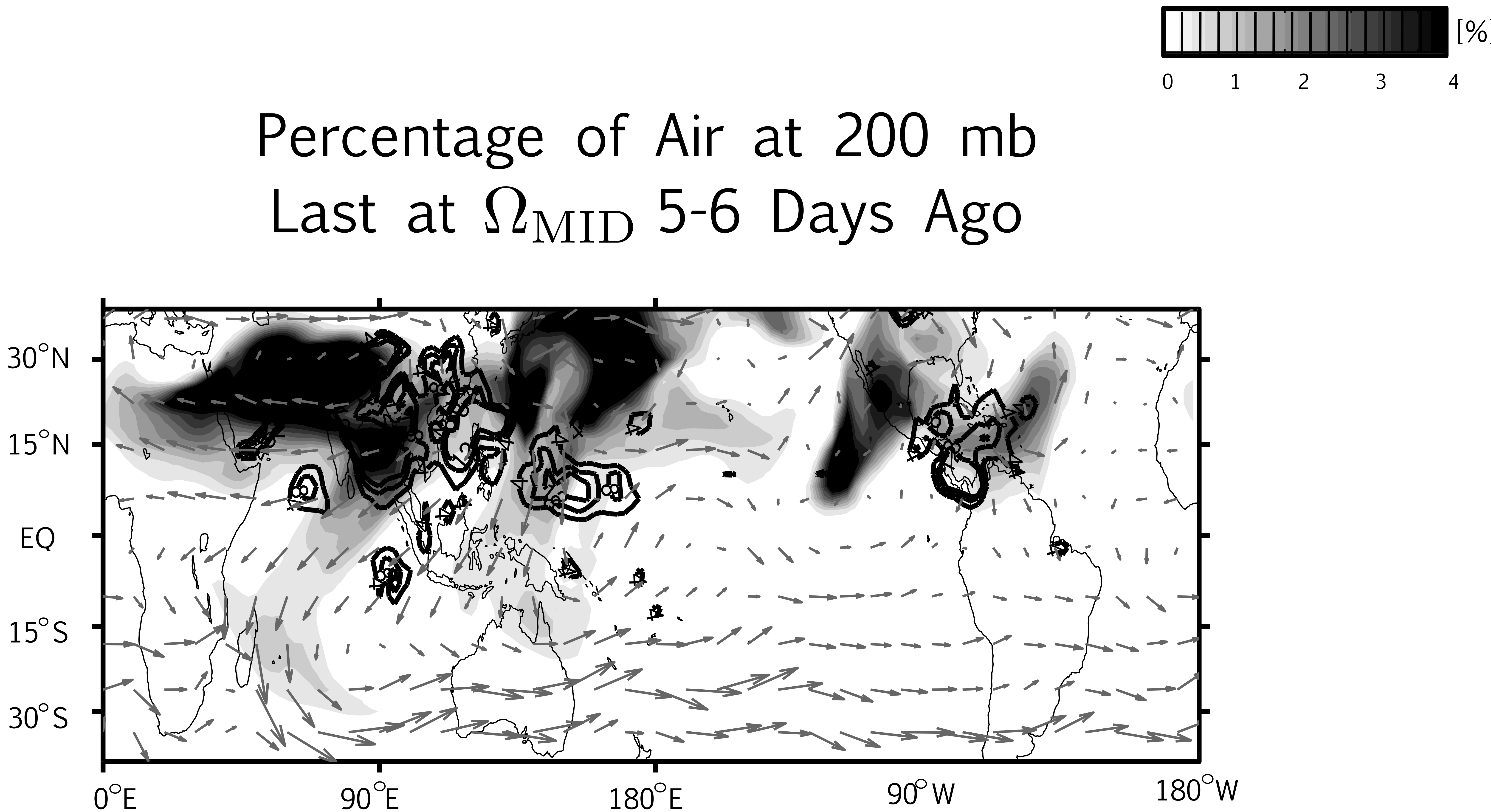

Shading: BIR fraction $f_{\tau_1}^{\tau_2}(\mathbf{r}|\Omega_{\mathrm{MID}}, t')$
Black contours: cumulative mass flux from convection $[\times 10^{-3}\ \mathrm{kg/m^2/s}]$
Winds: MERRA Reanalysis

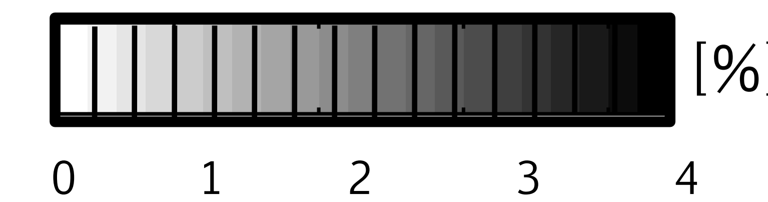

Percentage of Air at 200 mb
Last at Ω_{MID} 7-8 Days Ago

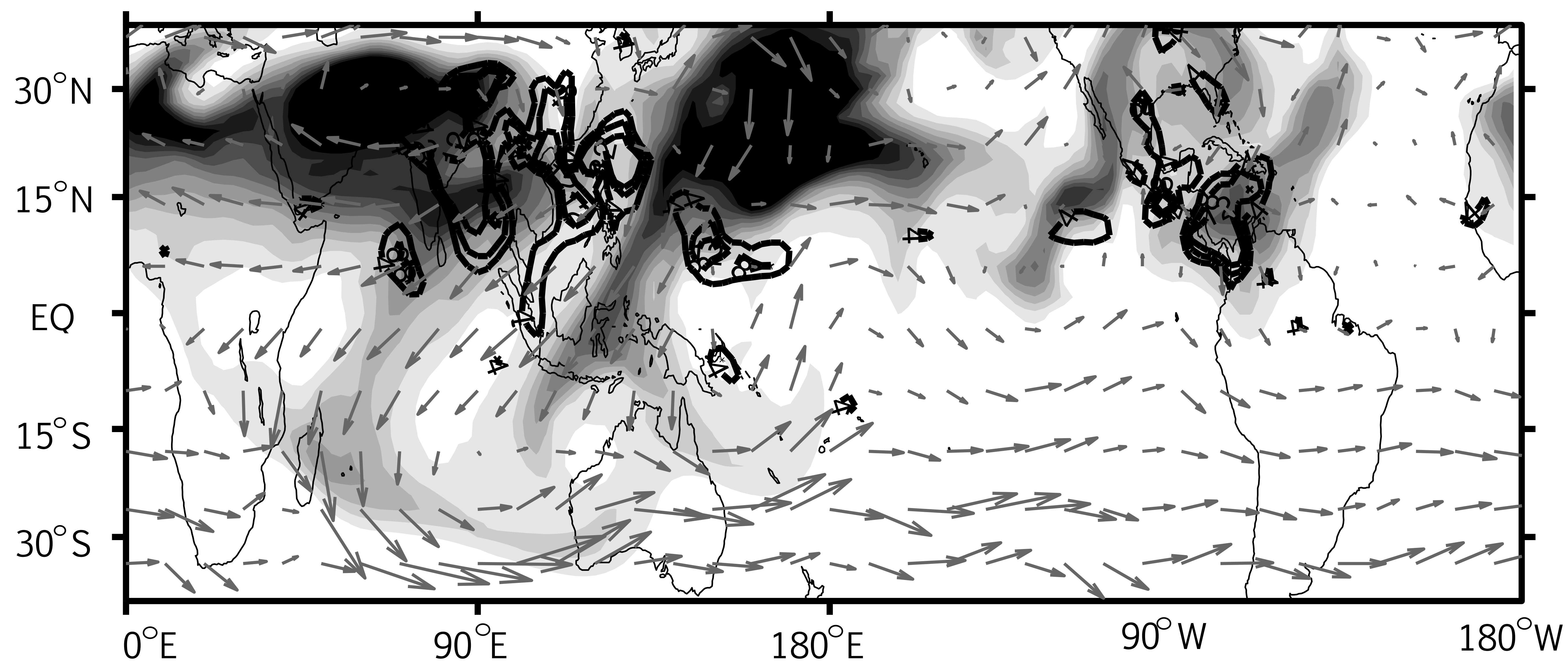

Shading: BIR fraction $f_{\tau_1}^{\tau_2}(\mathbf{r}|\Omega_{\mathrm{MID}}, t')$
Black contours: cumulative mass flux from convection $[\times 10^{-3}\ \mathrm{kg/m^2/s}]$
Winds: MERRA Reanalysis

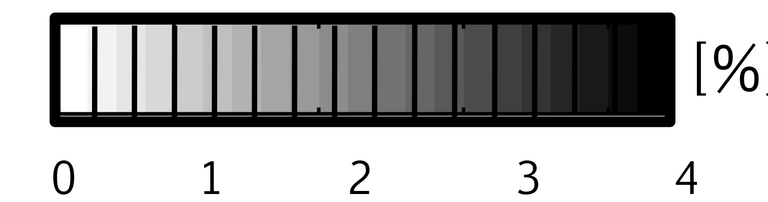

Percentage of Air at 200 mb Last at Ω_{MID} 5-6 Days Ago

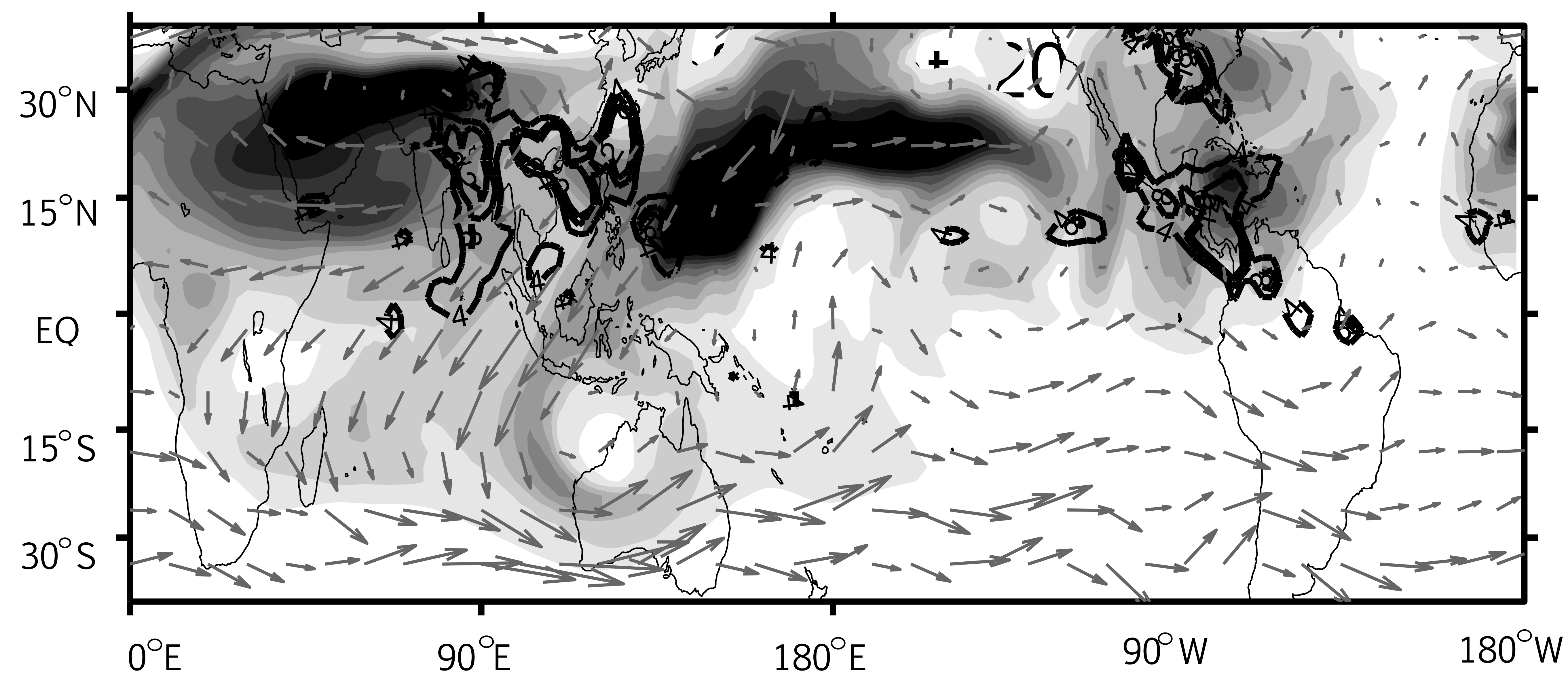

Shading: BIR fraction $f_{\tau_1}^{\tau_2}(\mathbf{r}|\Omega_{\mathrm{MID}}, t')$

Black contours: cumulative mass flux from convection $[\times 10^{-3}\ \mathrm{kg/m^2/s}]$

Winds: MERRA Reanalysis

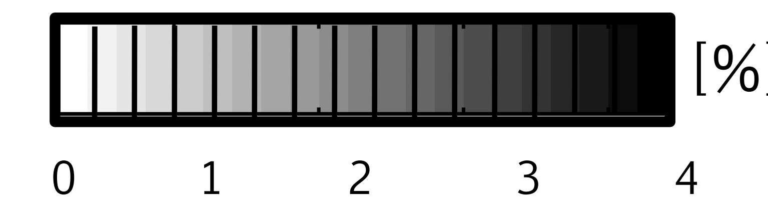

Percentage of Air at 200 mb Last at Ω_{MID} 11-12 Days Ago

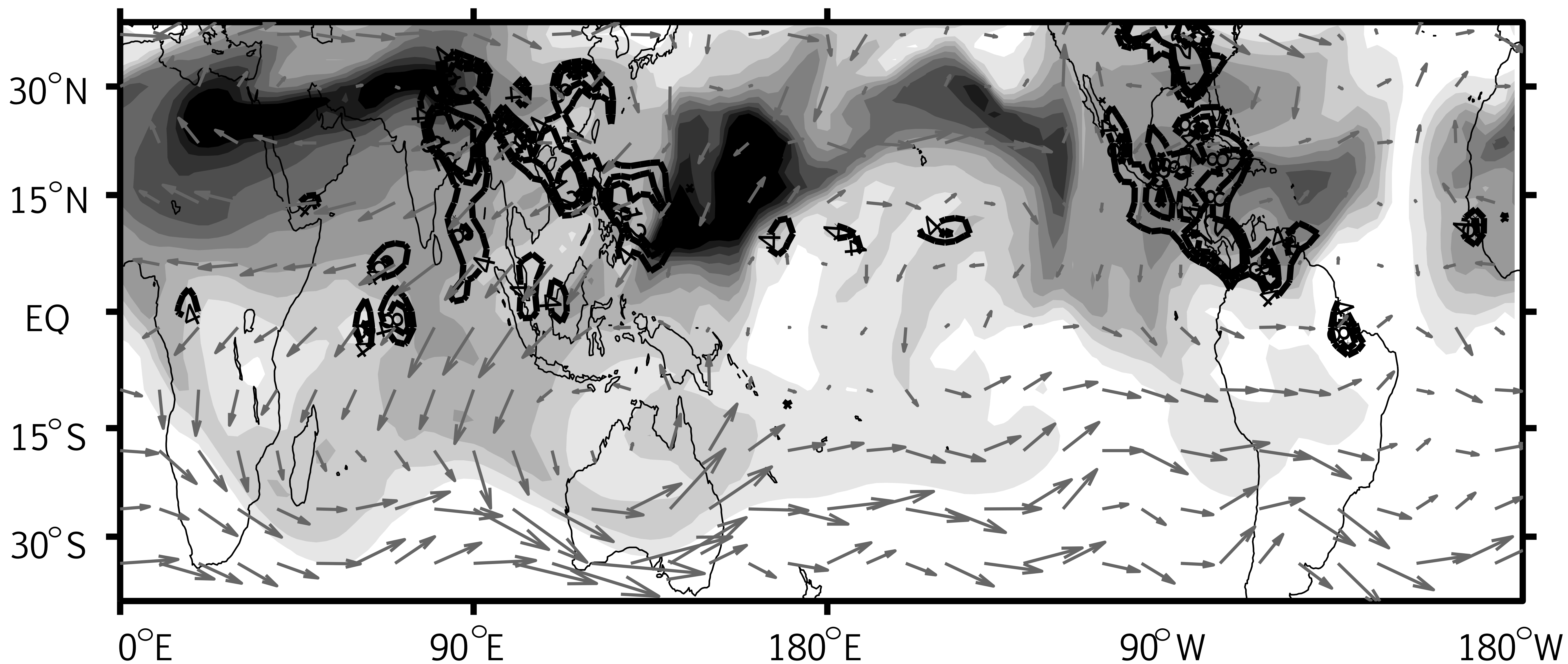

Shading: BIR fraction $f_{\tau_1}^{\tau_2}(\mathbf{r}|\Omega_{\mathrm{MID}}, t')$
Black contours: cumulative mass flux from convection $[\times 10^{-3}\ \mathrm{kg/m^2/s}]$
Winds: MERRA Reanalysis

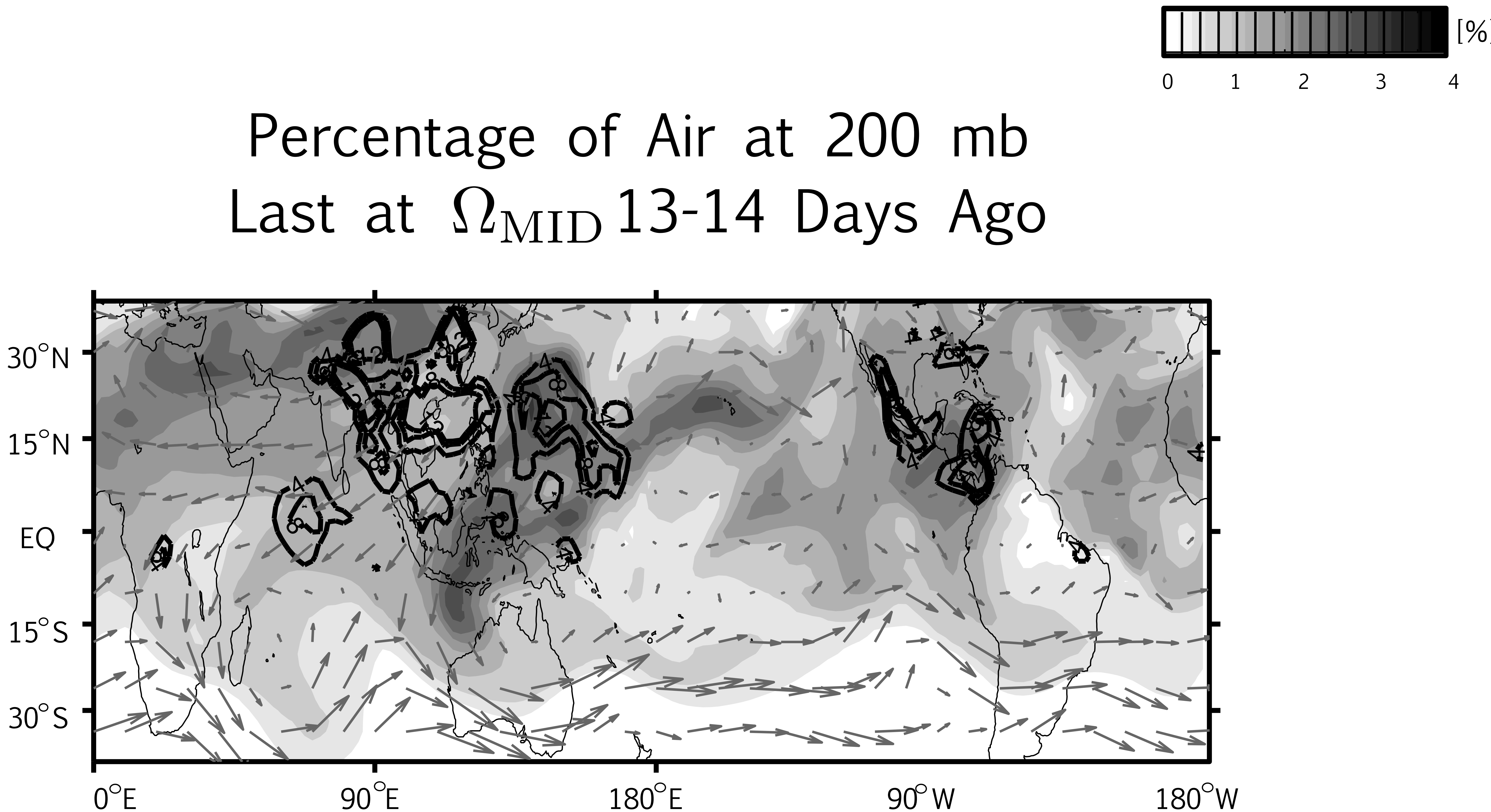

Shading: BIR fraction $f_{\tau_1}^{\tau_2}(\mathbf{r}|\Omega_{\mathrm{MID}}, t')$
Black contours: cumulative mass flux from convection $[\times 10^{-3}\ \mathrm{kg/m^2/s}]$
Winds: MERRA Reanalysis

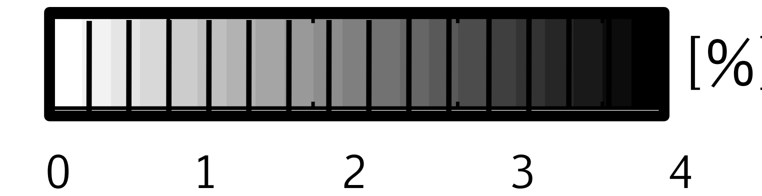

Percentage of Air at 200 mb
Last at Ω_{MID} 15-16 Days Ago

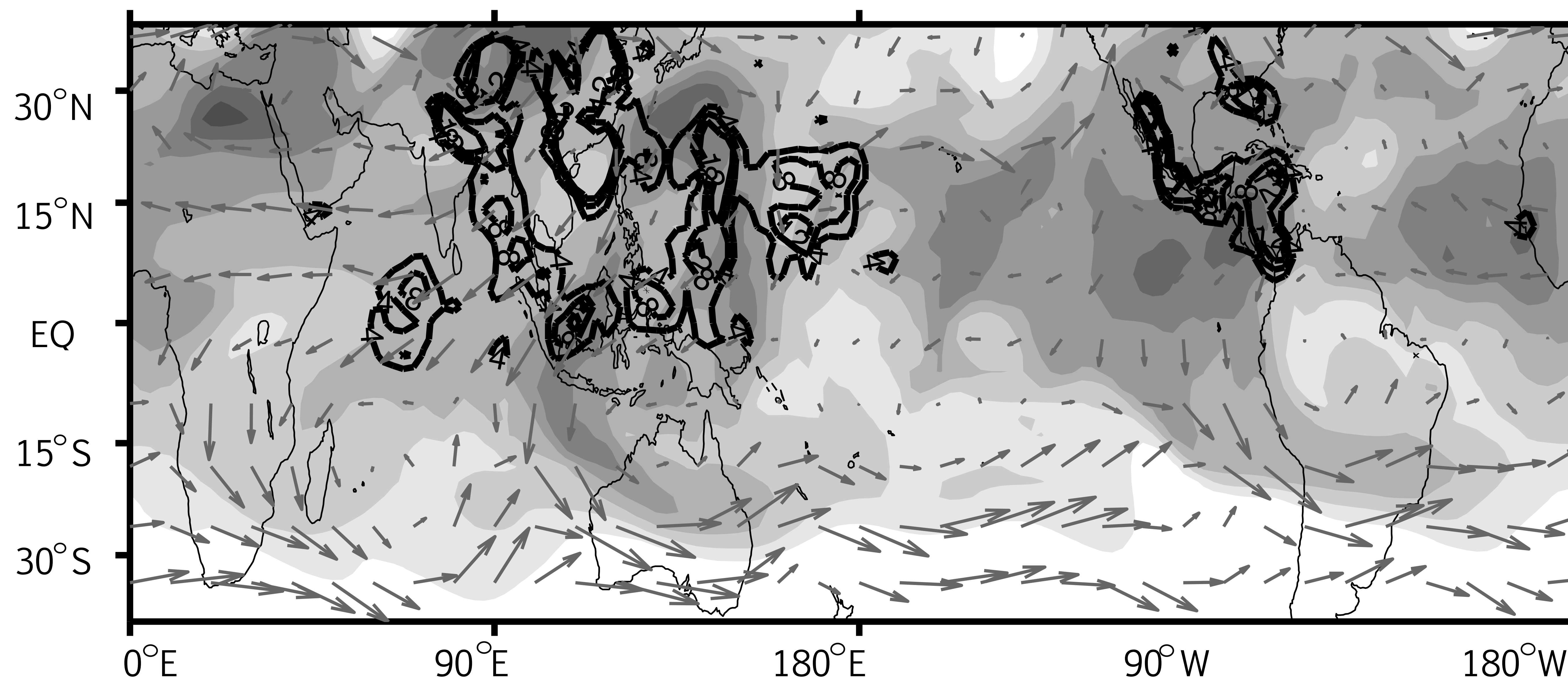

Shading: BIR fraction $f_{\tau_1}^{\tau_2}(\mathbf{r}|\Omega_{\mathrm{MID}}, t')$

Black contours: cumulative mass flux from convection $[\times 10^{-3}\ \mathrm{kg/m^2/s}]$

Winds: MERRA Reanalysis

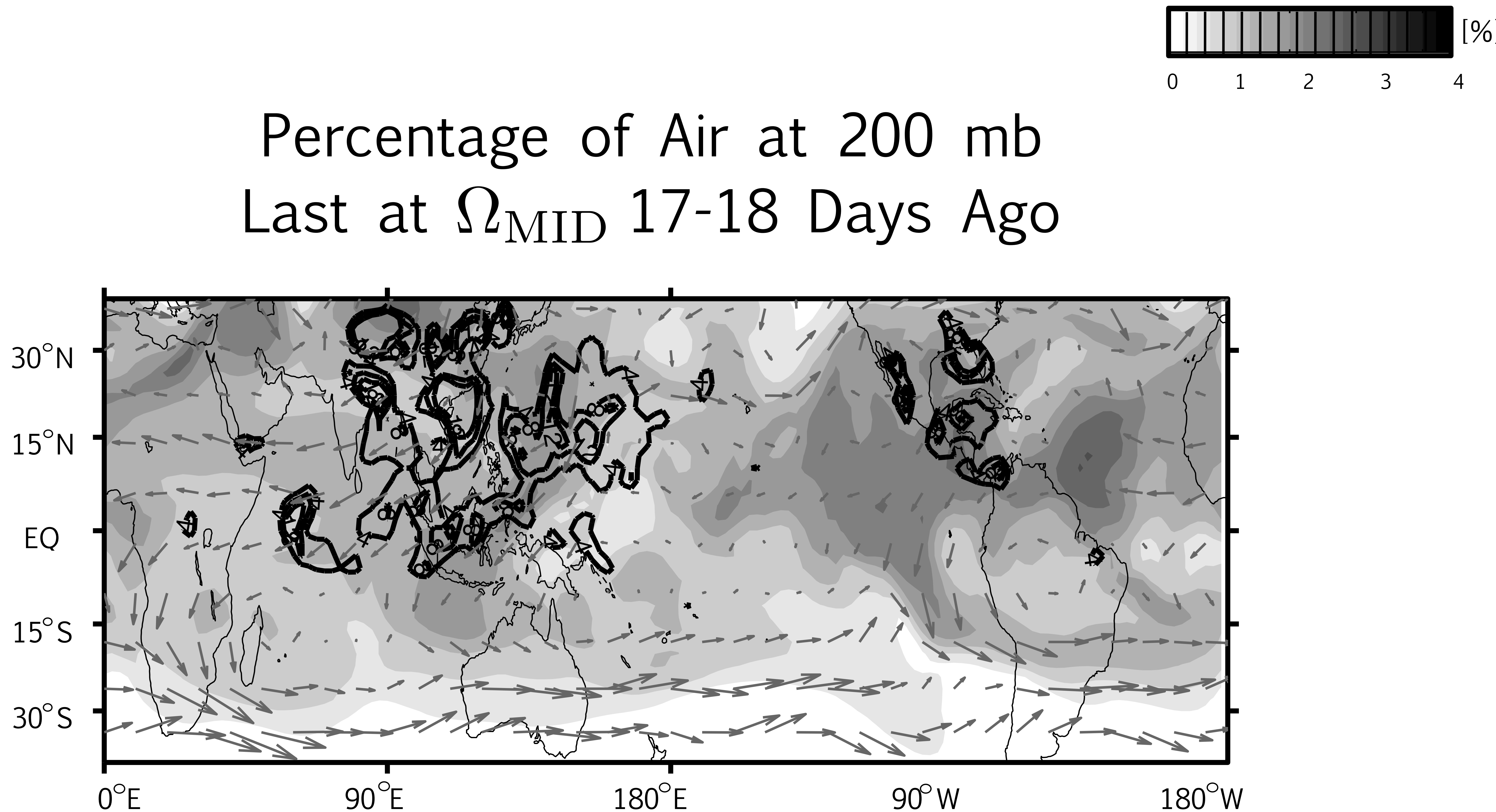

Shading: BIR fraction $f_{\tau_1}^{\tau_2}(\mathbf{r}|\Omega_{\mathrm{MID}}, t')$

Black contours: cumulative mass flux from convection $[\times 10^{-3}\ \mathrm{kg/m^2/s}]$

Winds: MERRA Reanalysis

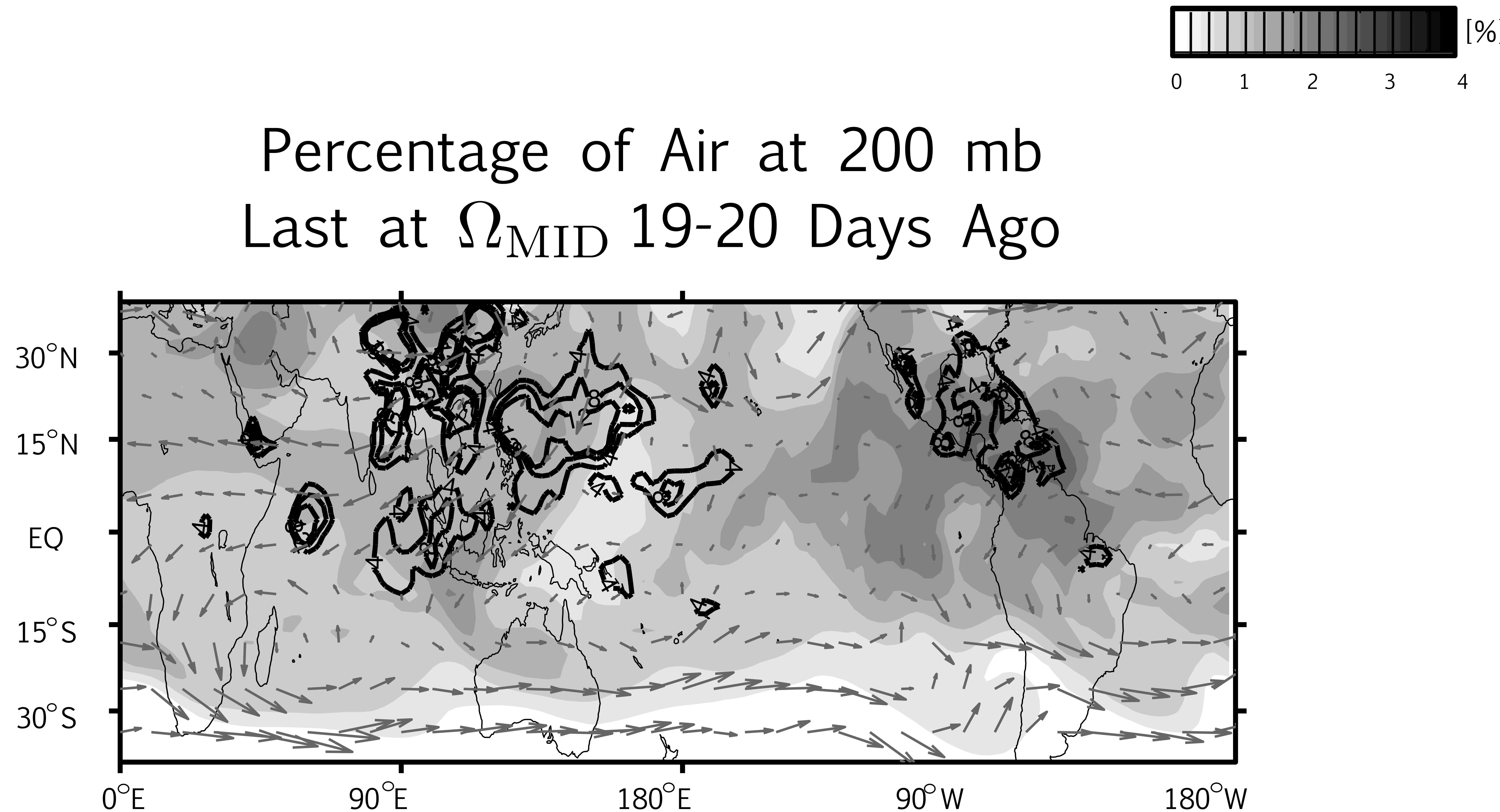

Shading: BIR fraction $f_{\tau_1}^{\tau_2}(\mathbf{r}|\Omega_{\mathrm{MID}}, t')$
Black contours: cumulative mass flux from convection $[\times 10^{-3}\ \mathrm{kg/m^2/s}]$
Winds: MERRA Reanalysis

While the TTD is a fundamental diagnostic of the flow it is ...

1) Not directly observable

2) Cumbersome to calculate properly in GCMS (i.e. non-stationary flows), unless an adjoint model is used (*Haine et al. (2008)*).

3) Approximation with BIRs cannot be used to give rigorous information about details of the seasonal and interannual variability of the TTD.

We know, however, the concentrations of chemically decaying species (χ_{τ_c}) emitted over Ω reflect the convolution of their loss (e.g. $e^{-\tau/\tau_c}$) with the underlying TTD, $\mathcal{G}(\tau)$.

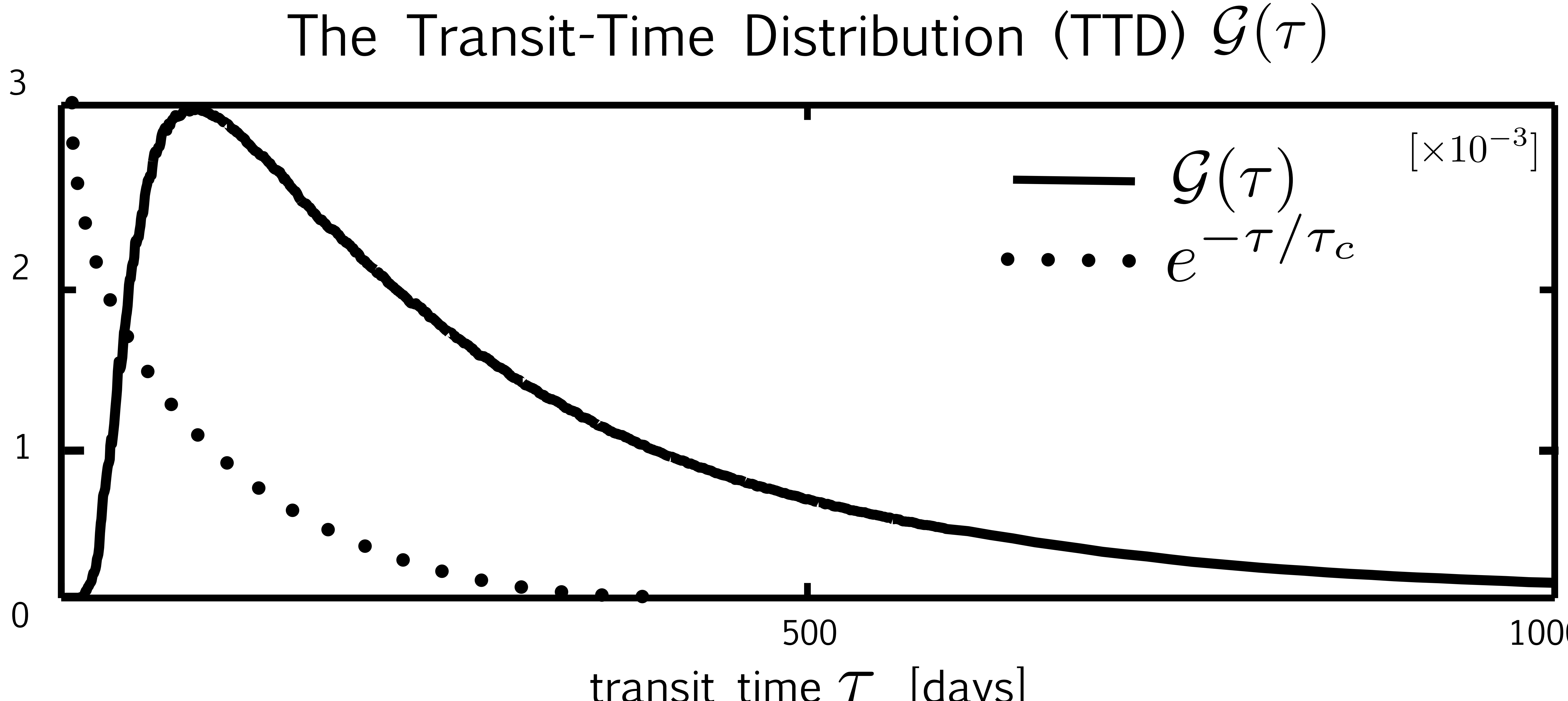

$$\chi_{\tau_c} = \int_0^{\infty} d\tau \; \chi_\Omega \mathcal{G}(\tau) e^{-\tau/\tau_c}$$

where χ_Ω = tracer concentration over source region

The Transit-Time Distribution (TTD) $\mathcal{G}(\tau)$

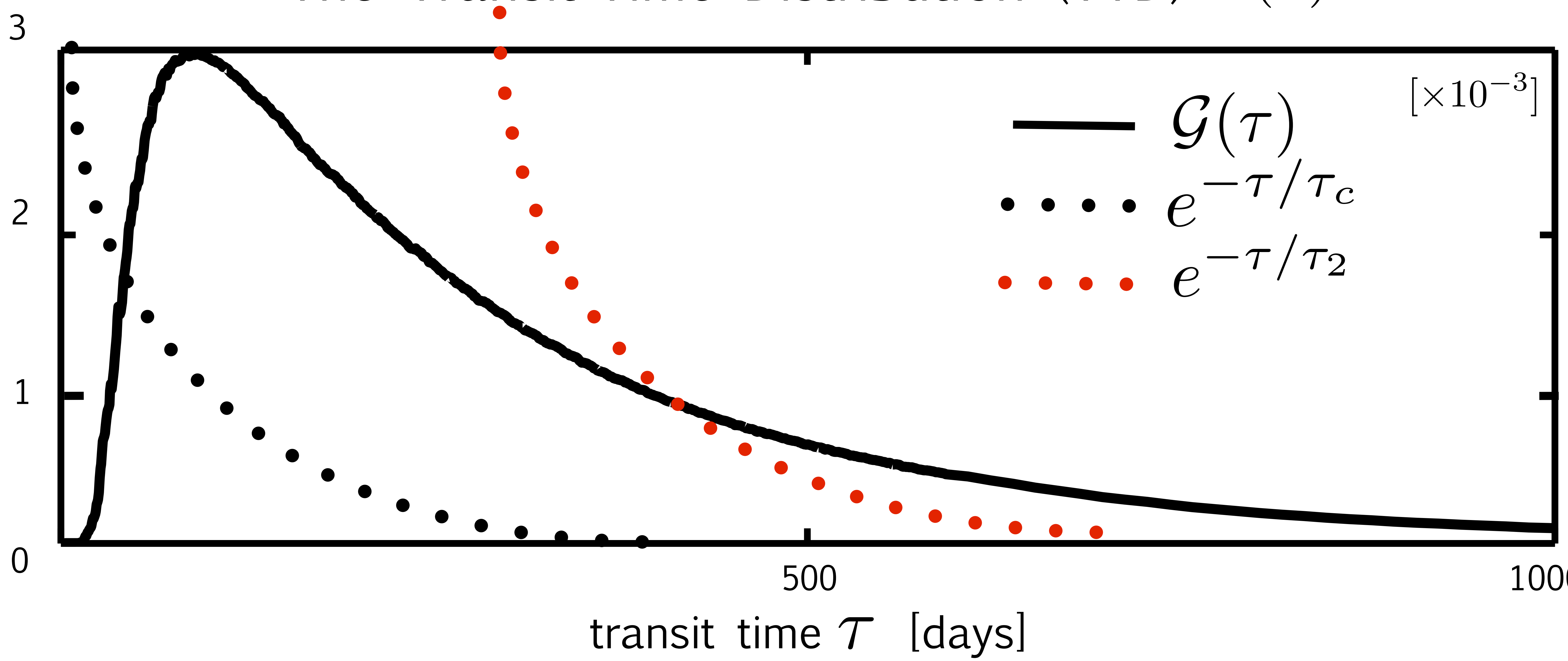

This suggests that combinations of tracers with different loss rates, τ_c^{-1}, can be used to infer the TTD in models.

It also suggests that real observable tracers (that undergo loss) can be used to constrain the TTD from observations.

A passive tracer (TR) suite has been introduced within the GEOS-5 model framework.

A subset of the TR tracers were also requested in the recent SPARC-IGAC Chemistry Climate Modeling Initiative (CCMI), enabling comparison of GEOS-5 atmospheric transport with broad range of other climate models.

Tracer (χ)	Boundary Condition ($\chi\Omega_{\mathrm{MID}}$)	Source (S)
NH Ideal (Mean) Age	0	1 year/year
NH-Loss (χ_{τ_c}) τ_c = 5, 50 days	1	$-\chi/\tau_c$

5-Day and 50-Day Tracers in GMI-MERRA Simulation

Annual Mean $\overline{\chi}^{*}_{\tau_c}$

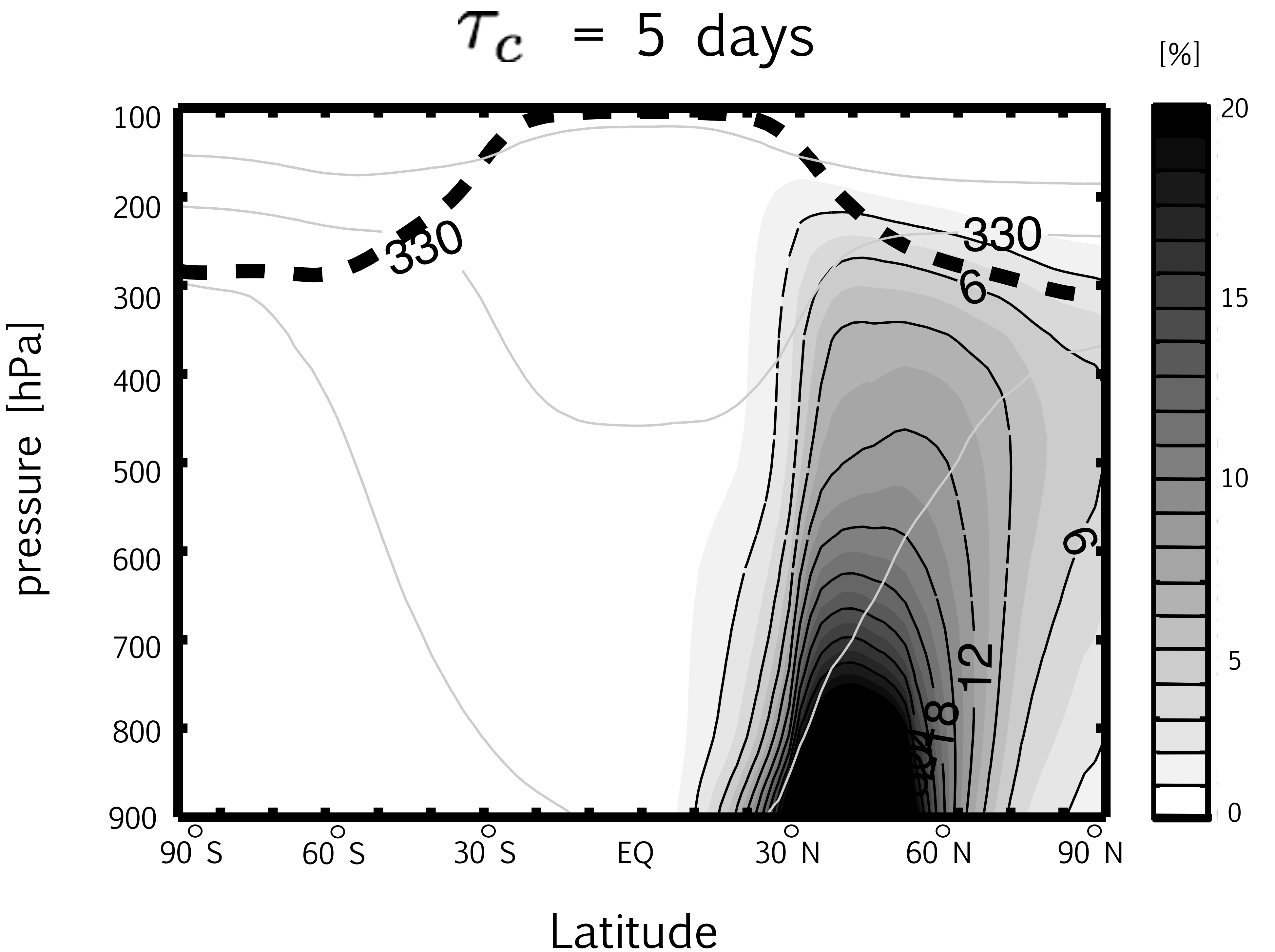

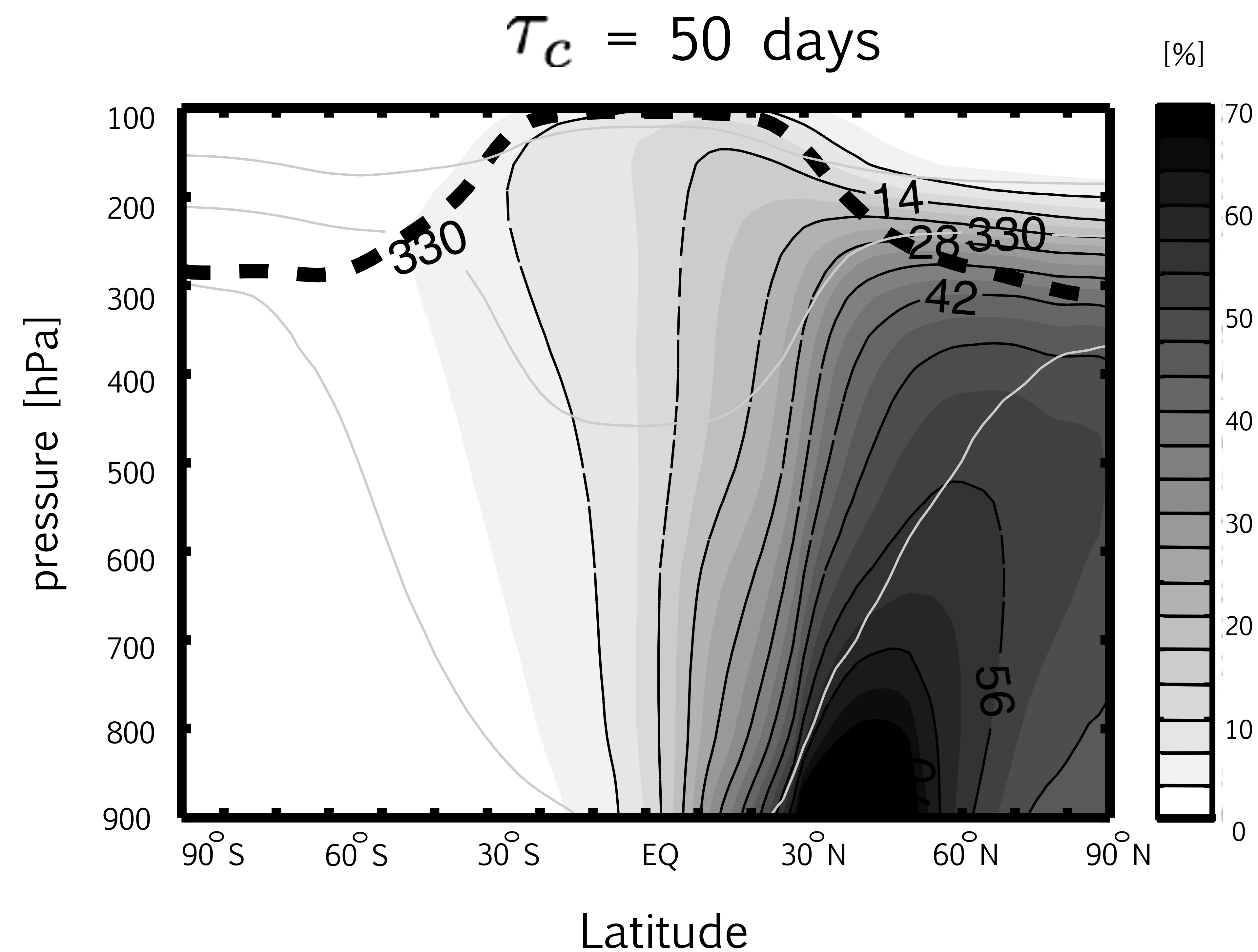

* 1980-2010 climatological mean, normalized by the tracer surface value (χ_Ω)

[Orbe et al. (2015), Submitted]

Direct Simulation of $\overline{\chi}^{*}_{\tau_c}$(top) vs. Reconstruction from TTD $\mathcal{G}(\tau)$(bottom)

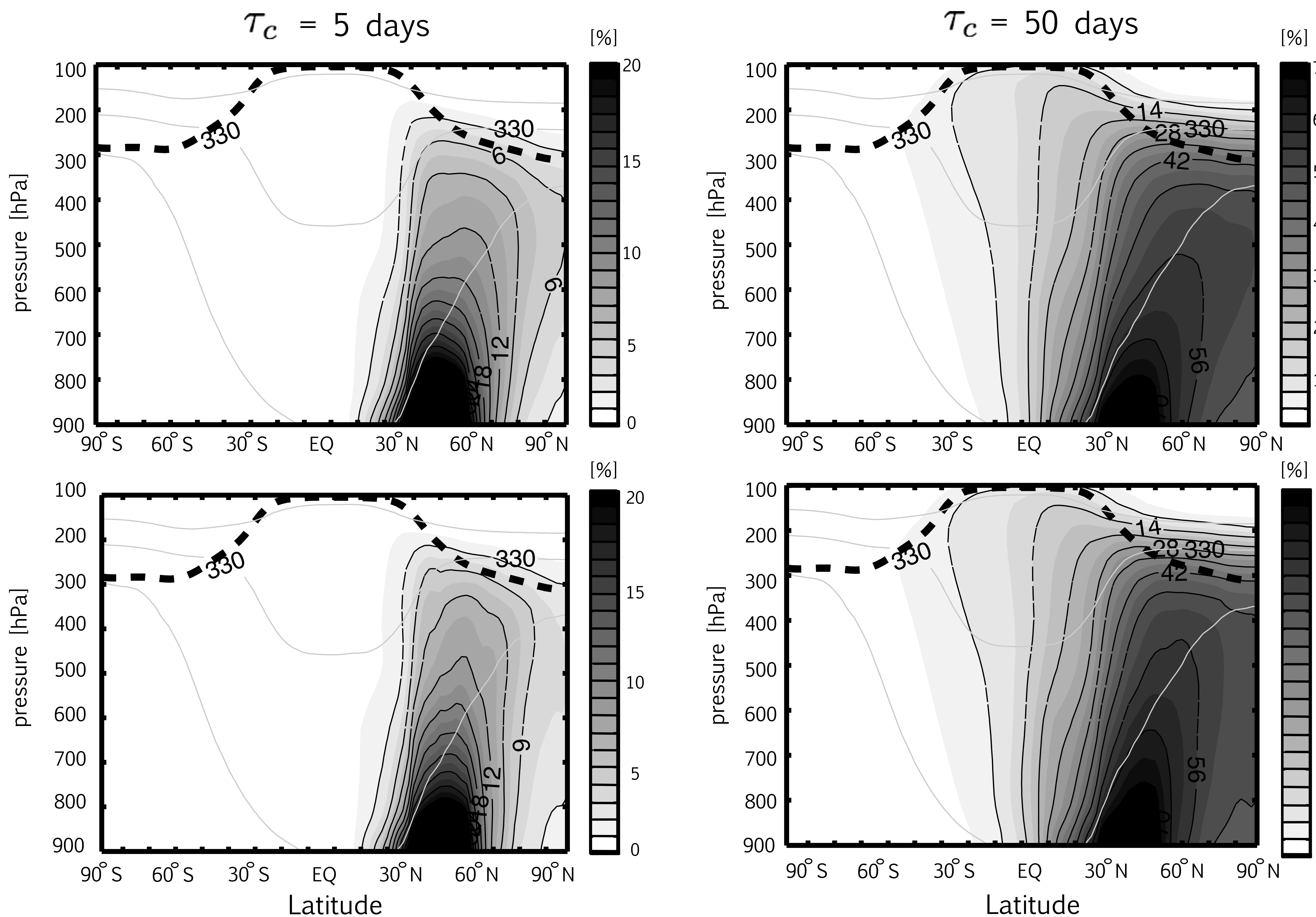

Fast Low-Level Transport Paths

Idealized loss tracers feature the low-level fast transport paths to the SH over the Pacific and Africa. Fast transport path signatures decrease with older tracer lifetimes. Here, the tracer age $\Gamma_{\tau_c} = -\tau_c \ln(\chi_{\tau_c}/\chi_{\Omega_{\mathrm{MID}}})$.

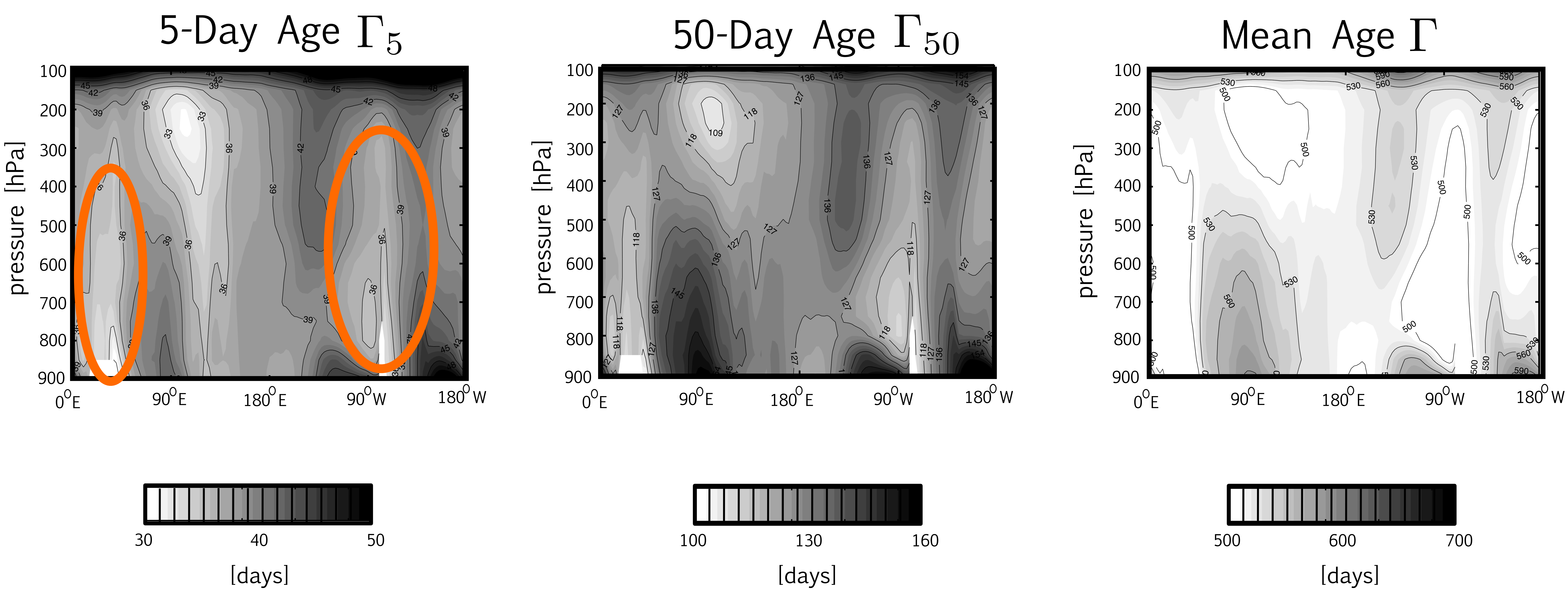

Fast Upper-Level Transport Paths South of the Asian Monsoon

Idealized loss tracers feature fast upper-level cross-equatorial transport paths over the Asian Monsoon and Pacific. Again, less structure in mean age tracer.

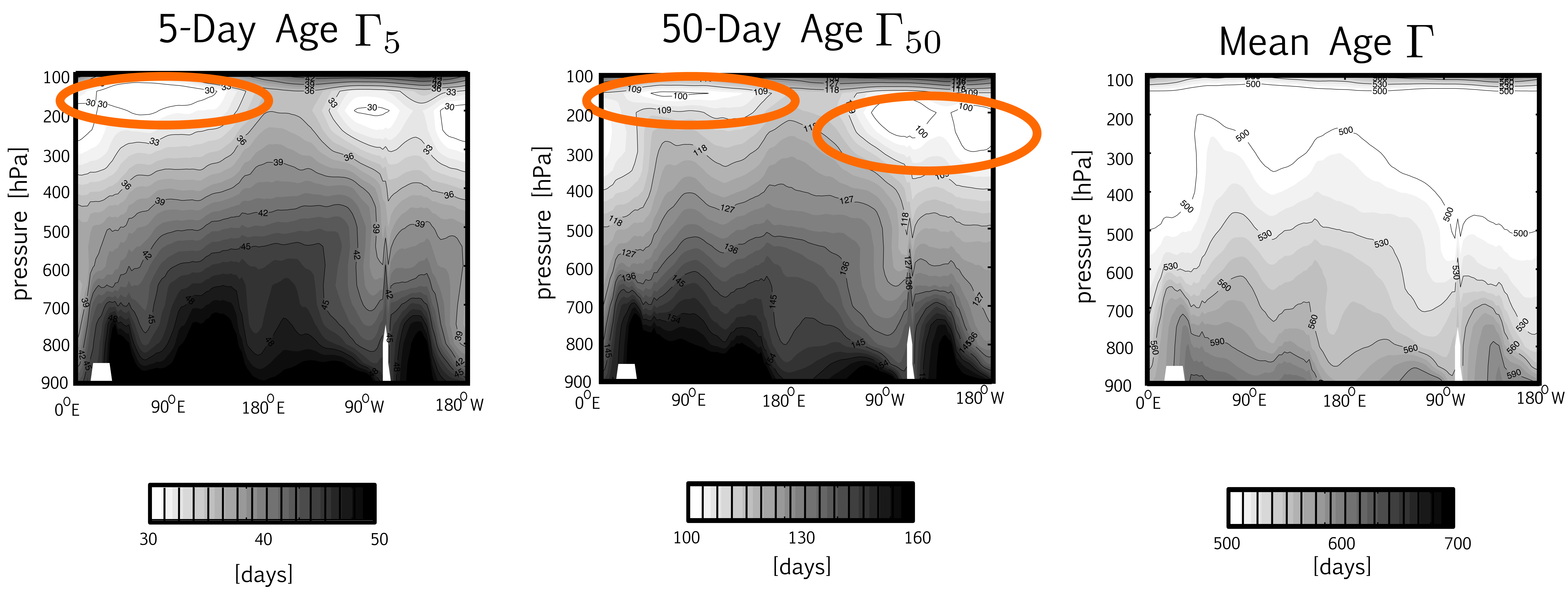

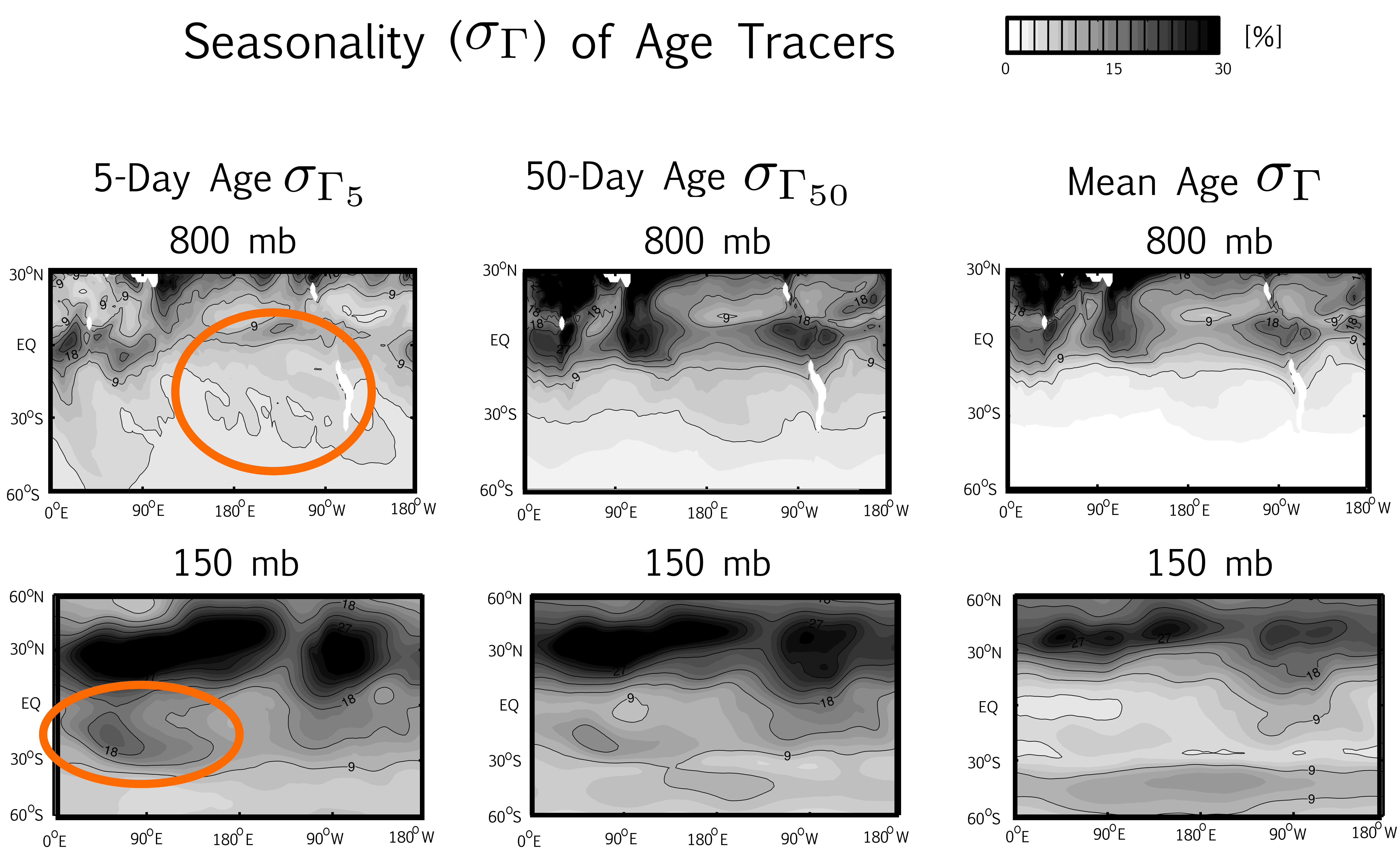
Seasonality (σ_Γ) of Age Tracers
[%]
0
15
30
5-Day Age σ_{Γ_5}
50-Day Age $\sigma_{\Gamma_{50}}$
Mean Age σ_Γ
800 mb
150 mb
30°N
EQ
30°S
60°S
60°N
0°E
90°E
180°E
90°W
180°W

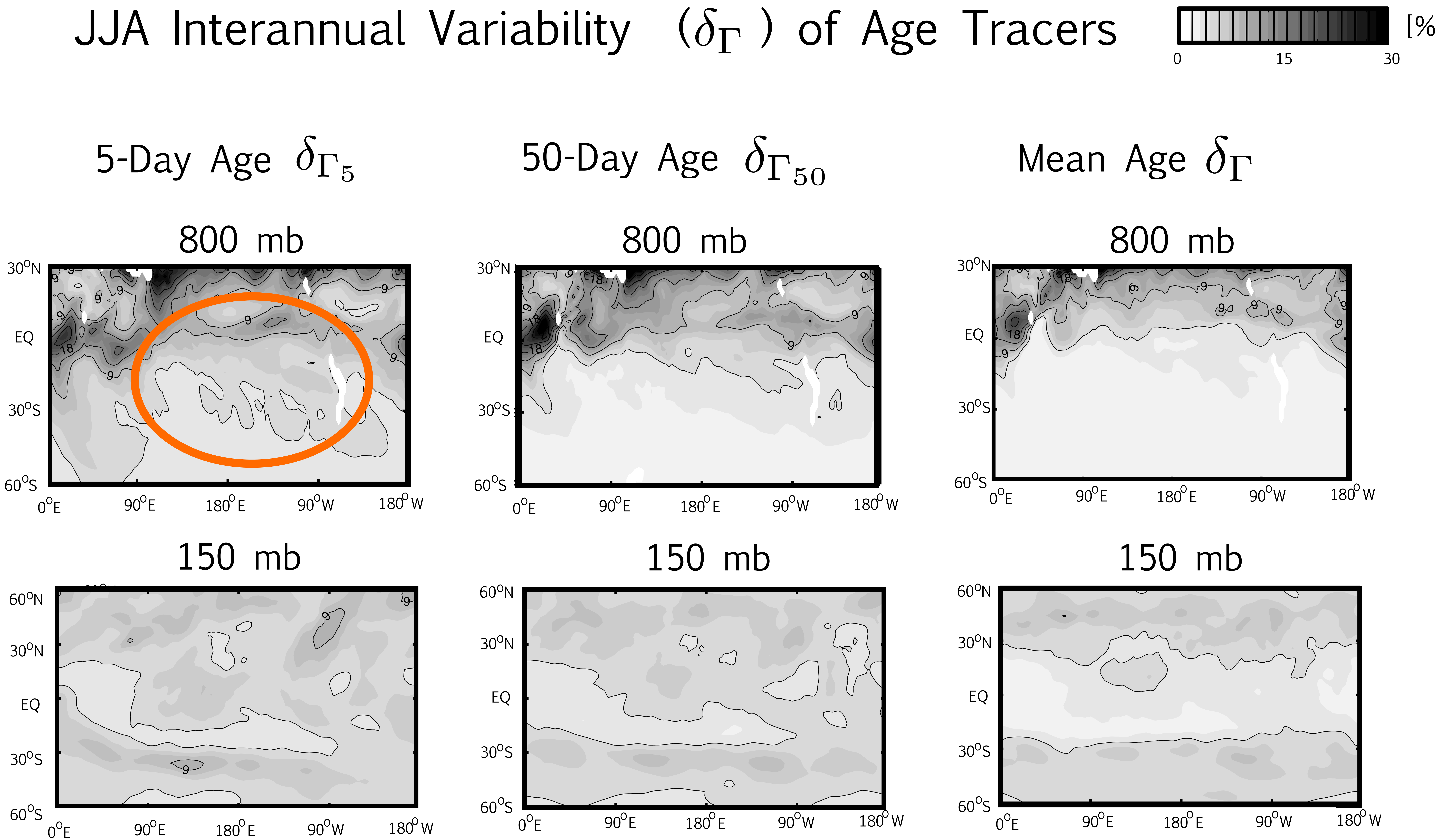
JJA Interannual Variability (δ_Γ) of Age Tracers
[%]
0
15
30
5-Day Age δ_{Γ_5}
50-Day Age $\delta_{\Gamma_{50}}$
Mean Age δ_Γ
800 mb
150 mb
30°N
EQ
30°S
60°S
60°N
0°E
90°E
180°E
90°W
180°W
9
18

Transport in Specified Dynamics and Free-Running Simulations

Simulations

Model	Horizontal Resolution	Meteorological Fields
Replay (Her. V4.2)	C48	MERRA
GMI-CTM	2°x 2.5°	MERRA
WACCM 5-hr	1.9°x 2.5°	Nudged-MERRA**
WACCM 50-hr	1.9°x 2.5°	Nudged-MERRA**
Free (Her. V4.2)	C48	Internally Generated
WACCM Free	1.9°x 2.5°	Internally Generated

Specified-Dynamics Simulations:

-Same large-scale flow (MERRA (1979-2010))

-Different model configuration (convective parameterization, "nudging" approach)

* Regular Replay used, but Intermittent Replay Simulation produces similar transport in troposphere

** to T, U, V, PS

Transport in Specified Dynamics and Free-Running Simulations

Simulations

Model	Horizontal Resolution	Meteorological Fields
Replay (Her. V4.2)	C48	MERRA
GMI-CTM	2°x 2.5°	MERRA
WACCM 5-hr	1.9°x 2.5°	Nudged-MERRA**
WACCM 50-hr	1.9°x 2.5°	Nudged-MERRA**
Free (Her. V4.2)	C48	Internally Generated
WACCM Free	1.9°x 2.5°	Internally Generated

Free-Running Simulations:

-Different large-scale flow

* Regular Replay used, but Intermittent Replay Simulation produces similar transport in troposphere

** to T, U, V, PS

Transport Differences: 5-Day Age

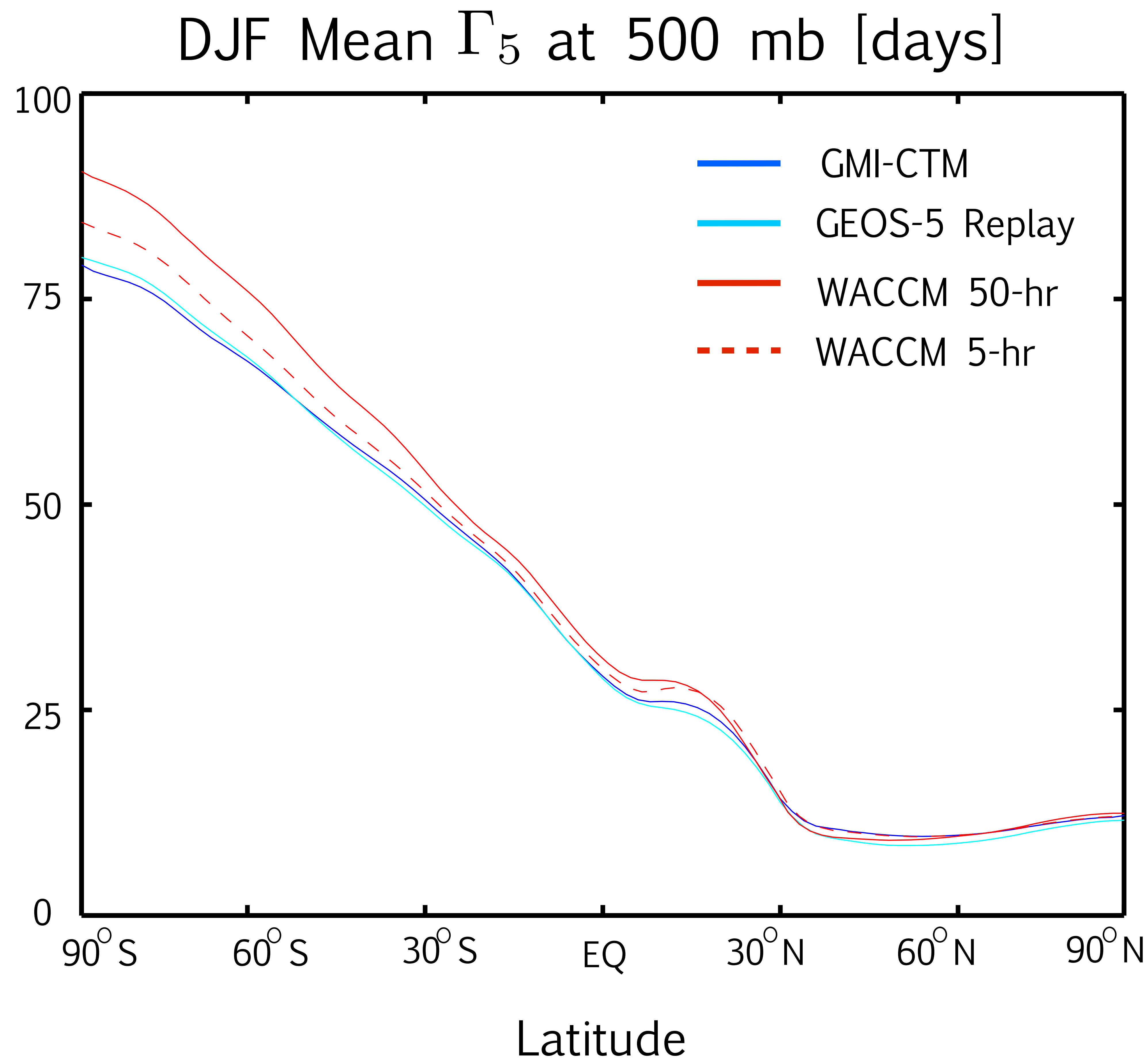

Transport Differences: 50-Day Age

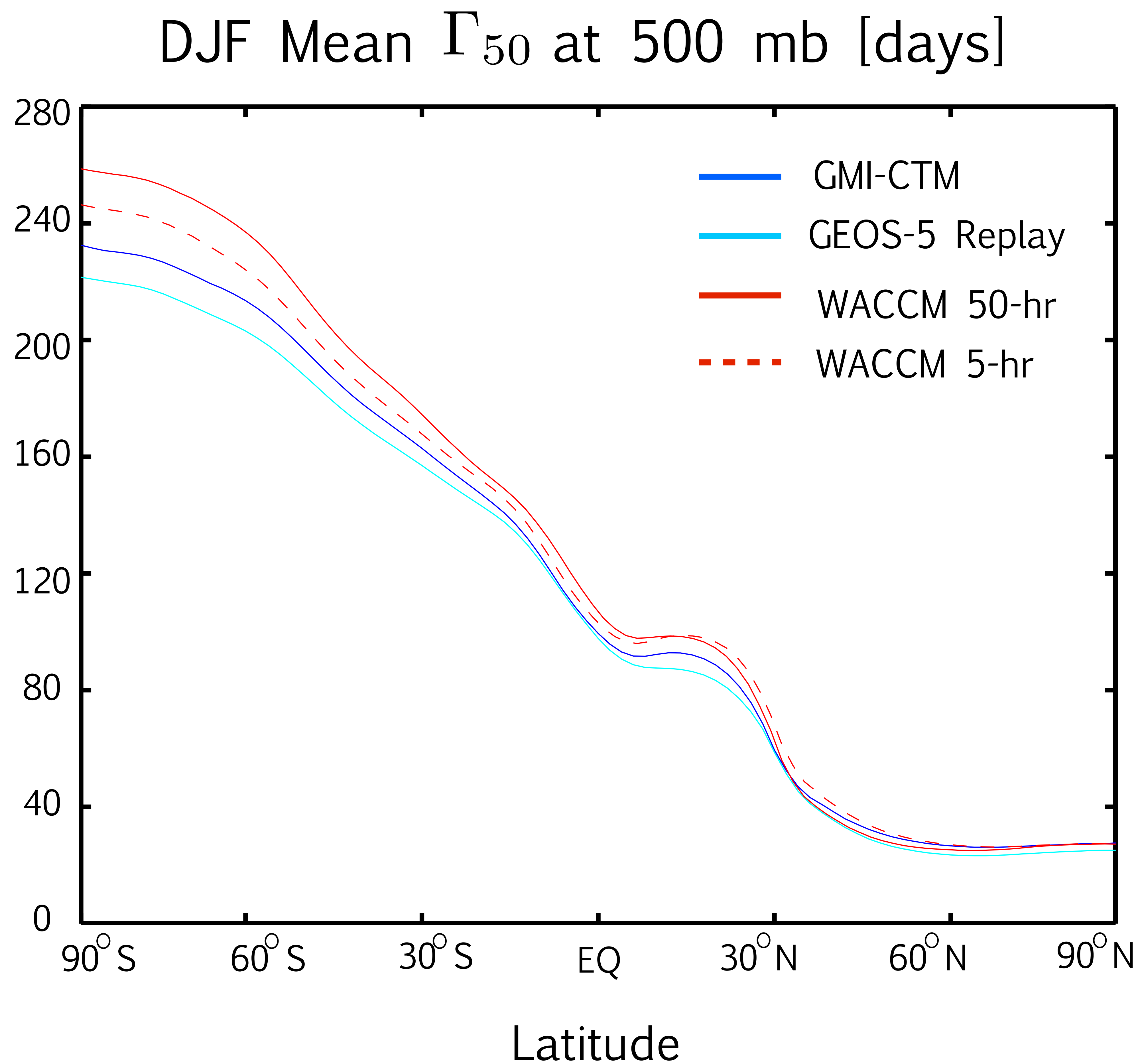

Transport differences between simulations amplify at longer transport timescales.

Transport Differences: Mean Age

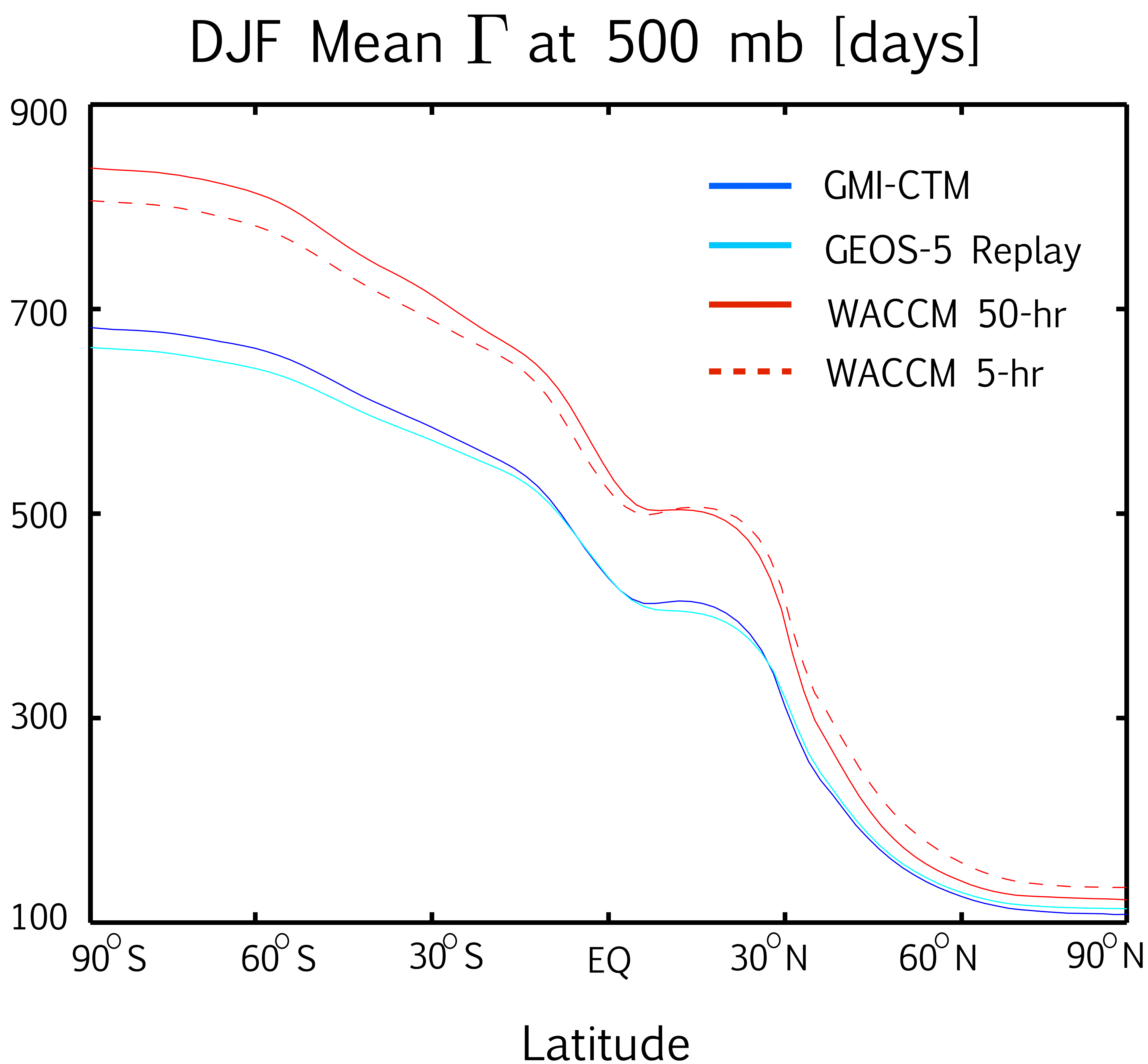

Transport differences between simulations amplify at longer transport timescales resulting in ~20-30% difference in interhemispheric transport between simulations with the *same large-scale flow.*

Source of Transport Differences: Tropical Convection

Cum. Mass Flux from Convection (CMF_CNV)
Evaluated over the Indian Ocean*

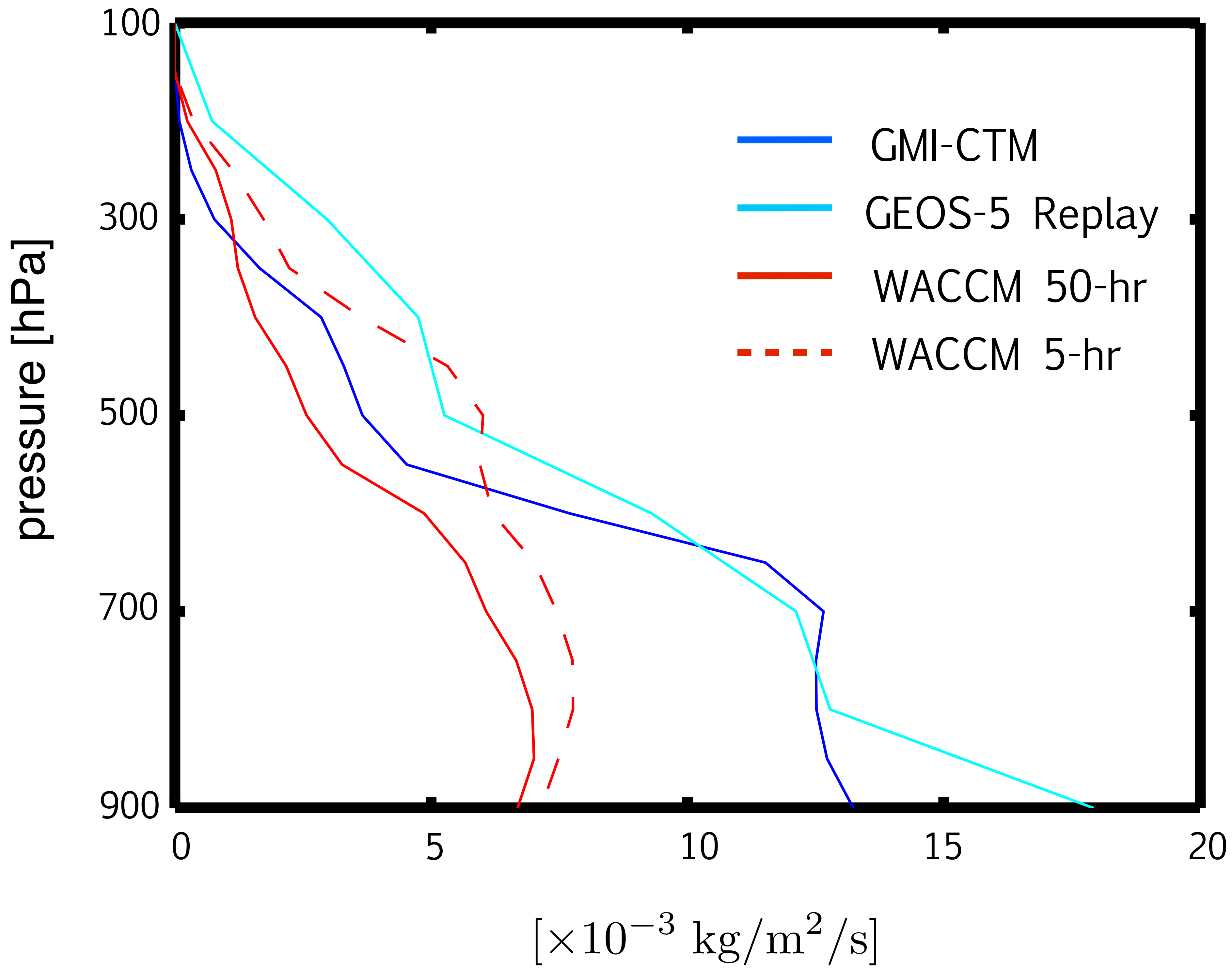

* = 800 mb, 60°E - 90°E between 5°S- 10°S

- Same large-scale flow but very different convective mass fluxes
- NASA models' convective mass fluxes are larger, especially in the lower troposphere.

Source of Transport Differences: Tropical Convection

Specified-Dynamics Simulations

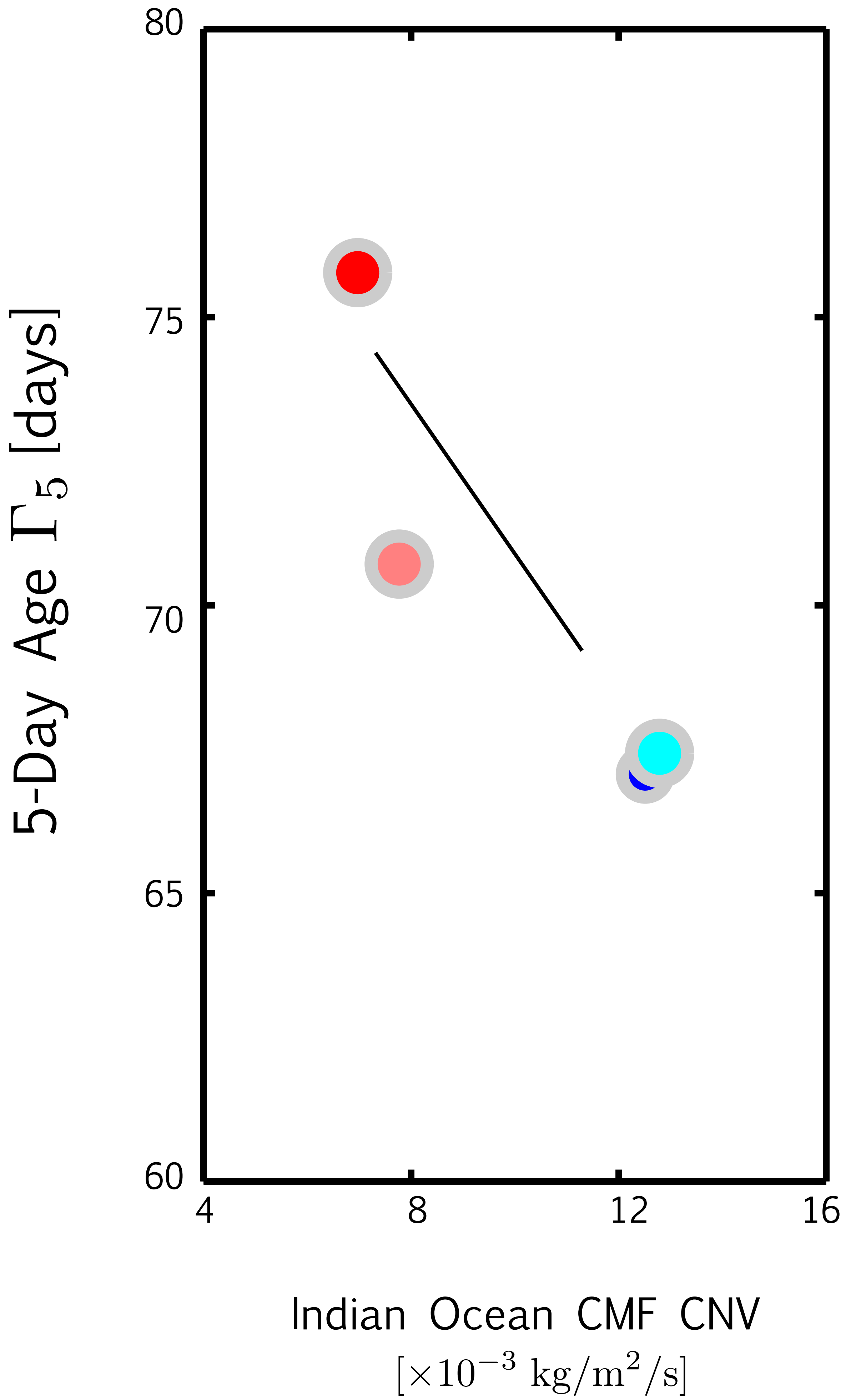

Stronger lower tropospheric tropical convection associated with younger ages in the SH (i.e. faster interhemispheric transport).

Source of Transport Differences: Tropical Convection

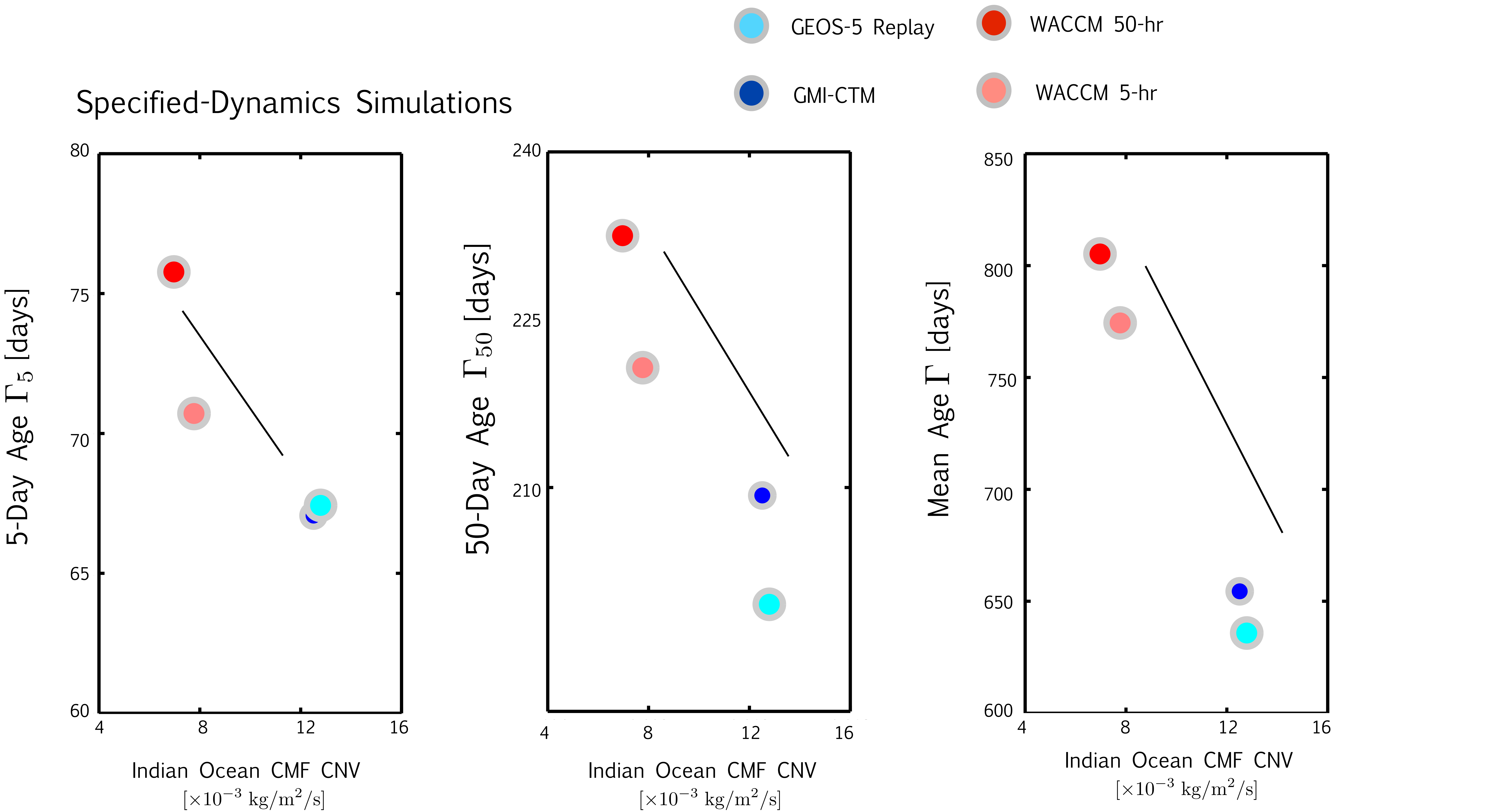

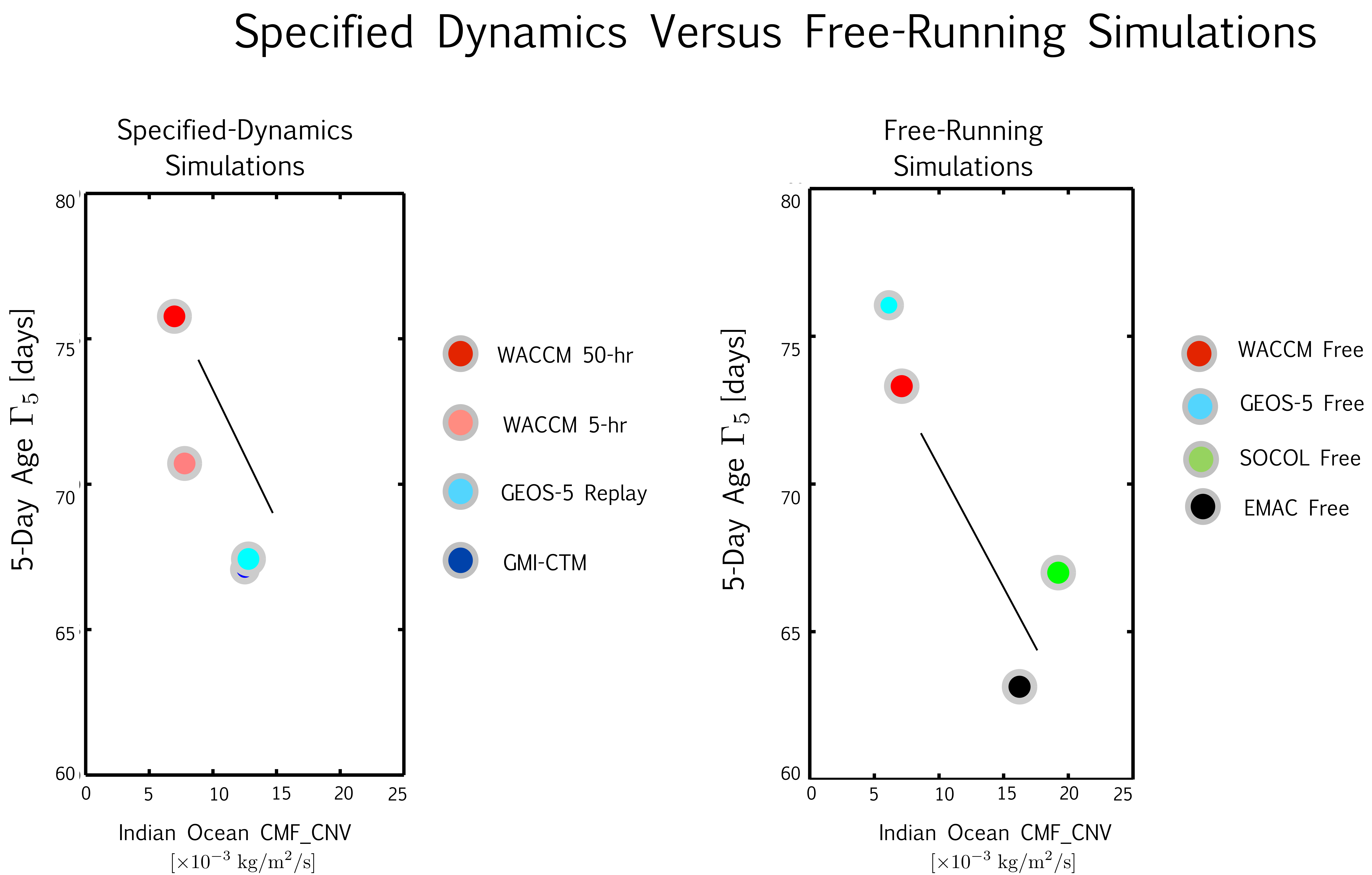

Specified Dynamics Versus Free-Running Simulations
Specified-Dynamics Simulations
Free-Running Simulations
5-Day Age Γ_5 [days]
Indian Ocean CMF_CNV
[$\times 10^{-3}$ kg/m^2/s]
WACCM 50-hr
WACCM 5-hr
GEOS-5 Replay
GMI-CTM
WACCM Free
GEOS-5 Free
SOCOL Free
EMAC Free

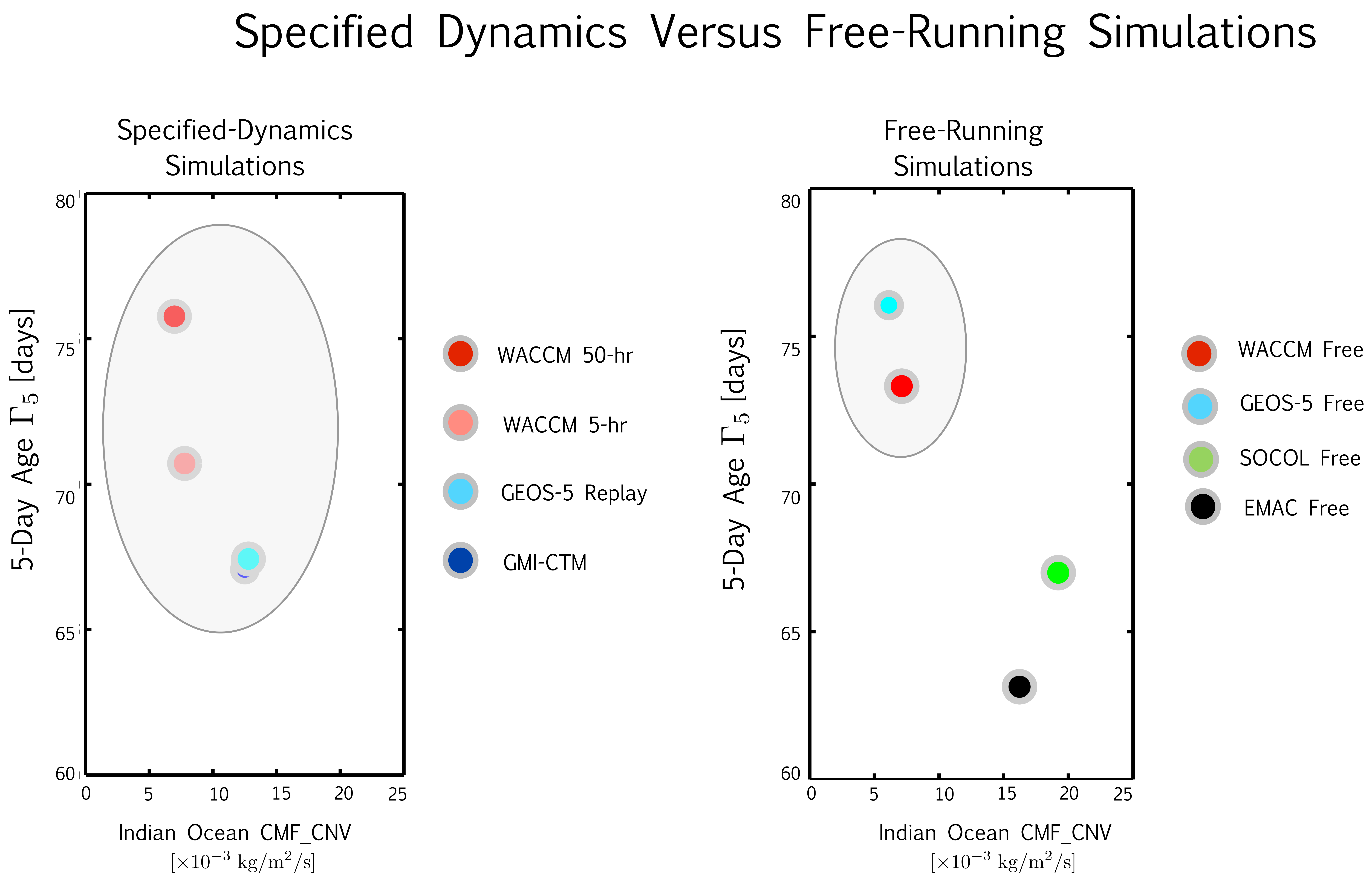

Specified Dynamics Versus Free-Running Simulations
Specified-Dynamics Simulations
5-Day Age Γ_5 [days]
80
75
70
65
60
0
5
10
15
20
25
Indian Ocean CMF_CNV
$[\times 10^{-3}\ \mathrm{kg/m^2/s}]$
WACCM 50-hr
WACCM 5-hr
GEOS-5 Replay
GMI-CTM
Free-Running Simulations
5-Day Age Γ_5 [days]
Indian Ocean CMF_CNV
$[\times 10^{-3}\ \mathrm{kg/m^2/s}]$
WACCM Free
GEOS-5 Free
SOCOL Free
EMAC Free

Conclusions

There is a broad distribution of transit times that controls transport from the NH midlatitude surface:

#1 Fast cross-equatorial transport paths are concentrated over the Pacific during DJF and south of the Asian Monsoon anticyclone during JJA.

#2 Time variations in idealized loss tracers reveal *large seasonality* and *weak interannual variability* in upper tropospheric fast cross-equatorial transport paths. Why?

Conclusions

Comparisons of large-scale interhemispheric transport between free-running and specified dynamics simulations show that:

#1 There are large (20-30%) differences in interhemispheric transport between models driven with the *same large scale flow*. The interhemispheric transport between free-running simulations is *more similar* than between specified dynamics simulations.

#2 These differences appear to be related to differences in convection in the tropics and its handling in various “nudged/replay” simulations.